Spatiotemporal Variability in the Oxidative Potential of Ambient Fine Particulate Matter in Midwestern United States

Haoran Yu[1], Joseph Varghese Puthussery[1], Yixiang Wang[1], Vishal Verma[1]*

[1]Department of Civil and Environmental Engineering, University of Illinois at Urbana-Champaign, Urbana, IL, 61801, United States

* *Correspondence to:* Vishal Verma (vverma@illinois.edu)

Abstract. We assessed the oxidative potential (OP) of both water-soluble and methanol-soluble fractions of ambient fine particulate matter ($PM_{2.5}$) in the midwestern United States. A large set of $PM_{2.5}$ samples (N = 241) were collected from five sites, setup in different environments, i.e. urban, rural and roadside, in Illinois, Indiana and Missouri during May 2018 – May 2019. Five acellular OP endpoints, including the consumption rate of ascorbic acid and glutathione in a surrogate lung fluid (SLF) (OP^{AA} and OP^{GSH}, respectively), dithiothreitol (DTT) depletion rate (OP^{DTT}), and ·OH generation rate in SLF and DTT ($OP^{OH\text{-}SLF}$ and $OP^{OH\text{-}DTT}$, respectively), were measured for all $PM_{2.5}$ samples. $PM_{2.5}$ mass concentrations in the Midwest US as obtained from these samples were spatially homogeneously distributed, while most OP endpoints showed significant spatiotemporal heterogeneity. Seasonally, higher activities occurred in summer for most OP endpoints for both water- and methanol-soluble extracts. Spatially, roadside site showed highest activities for most OP endpoints in the water-soluble extracts, while only occasional peaks were observed at urban sites in the methanol-soluble OP. Most OP endpoints showed similar spatiotemporal trends between mass- and volume-normalized activities across different sites and seasons. Comparisons between two solvents (i.e. water and methanol) showed that methanol-soluble OP generally had higher activity levels than corresponding water-soluble OP. Site-to-site comparisons of OP showed stronger correlations for methanol-soluble OP compared to water-soluble OP, indicating a better extraction of water-insoluble redox-active compounds from various emission sources into methanol. We found a weak correlation and inconsistent slope values between $PM_{2.5}$ mass and most OP endpoints. Moreover, the poor-to-moderate intercorrelations among different OP endpoints infer different mechanisms of OP represented by these endpoints, and thus demonstrate the rationale for analyzing multiple acellular endpoints for a better and comprehensive assessment of OP.

1 Introduction

Oxidative stress induced by ambient fine particulate matter ($PM_{2.5}$; particulate matter with size less than 2.5 μm) has been widely recognized as a biological pathway for fine particles to exert adverse health effect in humans (Sørensen et al., 2003;Risom et al., 2005;Garçon et al., 2006;Wessels et al., 2010;Cachon et al., 2014;Haberzettl et al., 2016;Feng et al., 2016;Rao et al., 2018;Mudway et al., 2020). A variety of chemical species in ambient particles, such as transition metals and aromatic organic species, possess redox cycling capability and can catalyze electron transfer from cellular reductants (e.g. NADPH) to molecular oxygen (O_2), which subsequently forms highly reactive radicals [e.g. superoxide radical ($\cdot O_2^-$) and hydroxyl radical (·OH)] and non-radical oxidants [e.g. hydrogen peroxide (H_2O_2)]

(Kampfrath et al., 2011;Qin et al., 2018;Kumagai et al., 2002;Lee et al., 2016). These oxygen containing species with high redox activity and short lifetime are collectively defined as the reactive oxygen species (ROS). Several antioxidants (e.g. ascorbic acid (AA), reduced glutathione (GSH) and uric acid (UA) etc.) that are present in human respiratory tract lining fluid (RTLF) can counteract the ROS under normal conditions by donating extra electrons, thus forming less-oxidative species and oxidized antioxidants (Kelly, 2003;Li and Nel, 2006;Allan et al., 2010;Zuo et al., 2013;Poljšak and Fink, 2014). However, excessively produced ROS might penetrate the antioxidant barrier and induce oxidative stress (Xing et al., 2016;Rao et al., 2018), leading to the cascade of detrimental biological effects such as oxidation of DNA, lipids and proteins (Rossner et al., 2008;Franco et al., 2008;Grevendonk et al., 2016), tissue injury (Feng et al., 2016;Gurgueira et al., 2002;Sun et al., 2020) and eventually cardiopulmonary impairment (Li et al., 2018;Kodavanti et al., 2000;Kampfrath et al., 2011). The capability of particulate matter (PM) for catalyzing the generation of ROS and/or the depletion of antioxidants is defined as the oxidative potential (OP) of PM (Bates et al., 2019).

The assessment of $PM_{2.5}$-induced oxidative stress is conventionally carried out through biological tests, including both *in vitro* (Becker et al., 2005;Zhang et al., 2008;Oh et al., 2011;Yan et al., 2016;Abbas et al., 2016;Deng et al., 2013) and *in vivo* designs (Kleinman et al., 2005;Riva et al., 2011;Pei et al., 2016;Araujo et al., 2008;Xu et al., 2011;Sancini et al., 2014). Although, these biological tests are highly relevant in terms of representing the health effects in humans, the time- and labor-intensive protocols as well as the cost of experimental materials generally limit their application to only small sample sizes. Various acellular chemical assays which assess the OP by replicating intrinsic biological mechanisms were therefore developed as alternatives. These assays are generally divided in two categories. The OP analysis approaches in the 1st category directly probe the generation of ROS during redox cycling reactions in presence of PM, such as the measurement of H_2O_2 and ·OH production in surrogate lung fluid (SLF) (Vidrio et al., 2009;Shen et al., 2011;Charrier et al., 2014;Ma et al., 2015), and H_2O_2 and ·OH production in dithiothreitol (DTT) (Yu et al., 2018;Xiong et al., 2017;Chung et al., 2006;Kumagai et al., 2002). The assays in 2nd category utilize the consumption of antioxidants such as AA (Visentin et al., 2016;Weichenthal et al., 2016b) and GSH (Künzli et al., 2006;Szigeti et al., 2016), or surrogates of cellular reductants such as DTT (Verma et al., 2014;Cho et al., 2005), as the OP indicator. Analyzing each PM sample for all of these chemical assays is also time-consuming. To address this concern, we have previously developed an automated OP analysis instrument named SAMERA – Semi-Automated Multi-Endpoint ROS-activity Analyzer, which can measure five most commonly used OP endpoints (i.e. consumption rate of AA and GSH in SLF, OP^{AA} and OP^{GSH} respectively; consumption rate of DTT, OP^{DTT}, and generation rate of ·OH in SLF and DTT, $OP^{OH\text{-}SLF}$ and $OP^{OH\text{-}DTT}$) for a PM extract in less than 3 hours (Yu et al., 2020). ~~These~~ Many of these acellular endpoints have been widely implemented by various researchers for assessing the oxidative properties of $PM_{2.5}$. Calas et al. (2018) compared the responses of several OP endpoints [i.e. OP^{DTT}, OP^{AA}, OP^{GSH}, and electron spin resonance (OP^{ESR})] on PM_{10} samples (N = 98) collected from Chamonix (France). Yang et al. (2014) also used four OP endpoints [OP^{AA}, OP^{DTT}, OP^{ESR} and reductive acridinium triggering (OP^{CRAT})] to investigate the effect of different extraction solvents and filter types on OP responses using the $PM_{2.5}$ samples (N = 20) collected from two cities (Rotterdam and Amsterdam) in Netherland. The comparison of OP^{AA}, OP^{DTT} and OP^{GSH} has been shown in two studies (Fang et al., 2016;Gao et al., 2020a), both from the southeast US. We are not aware of any study which has compared ·OH

generation in SLF or DTT with other endpoints based on antioxidants consumption (e.g. AA or GSH consumption). Clearly, the studies systematically comparing the responses of these different endpoints on a large sample-set collected from an extensive spatial scale, particularly in the United States are very limited. ~~However, there has not been a single study which has systematically compared the responses of all of these chemical assays in a single investigation.~~

Although OP is proposed as an integrative $PM_{2.5}$ property, purportedly combining the individual and synergistic actions of its many active components, there have been limited attempts to integrate it in the large-scale epidemiological studies. This is because, unlike other PM properties such as mass, sulfate, nitrate etc., the OP measurements in different geographical regions have been relatively sparse. Moreover, before integrating OP in the epidemiological studies, it is important that we investigate the differences of its spatiotemporal distribution with other commonly measured PM properties such as mass. An understanding of the temporal variation of OP in a specific environment could be helpful in time series studies of short-term effects, while the spatial variation of OP can aid in studying the long-term health effects of $PM_{2.5}$ exposure among different regions (Yang et al., 2015a). Globally, the spatiotemporal profiles of OP have been characterized for some geographical regions such as Los Angeles Basin (Saffari et al., 2014, 2013), Denver (Zhang et al., 2008), Atlanta (Fang et al., 2016;Verma et al., 2014) in US, Ontario (Canada) (Jeong et al., 2020;Weichenthal et al., 2019;Weichenthal et al., 2016a), France (Borlaza et al., 2021;Calas et al., 2019;Weber et al., 2018;Weber et al., 2021), Italy (Cesari et al., 2019;Perrone et al., 2019;Pietrogrande et al., 2018), Athens in Greece (Paraskevopoulou et al., 2019), Netherland (Yang et al., 2015a;Yang et al., 2015b), and some coastal cities of Bohai [Jinzhou, Tianjin and Yantai (Liu et al., 2018)] and Beijing (Yu et al., 2019;Liu et al., 2014) in China. Some of these studies have substantially contributed in enhancing our understanding of the role of OP in the PM-induced health effects (Fang et al., 2016;Tuet et al., 2016;Abrams et al., 2017;Weichenthal et al., 2016a;Yang et al., 2016;Bates et al., 2015). However, despite including many cities ranked high in terms of the air pollution [e.g. Indianapolis (Rosenthal et al., 2008), Chicago (Dominici et al., 2003), St. Louis (Sarnat et al., 2015), Detroit (Zhou et al., 2011), Cincinnati (Kaufman et al., 2019), and Cleveland (Kumar et al., 2013)], the midwestern region of the United States is an understudied region in terms of assessing the oxidative levels of ambient $PM_{2.5}$.

Here, we investigate the detailed spatiotemporal profiles of ambient $PM_{2.5}$ mass concentrations and OP in the midwestern United States. Simultaneous ambient $PM_{2.5}$ samples were collected from five different sites in the Midwest US. The automated instrument – SAMERA facilitated the measurement of OP on our large bulk of $PM_{2.5}$ samples (N = 241) collected from all the sites, which were extracted in both water and methanol separately. ~~This paper mainly discusses the spatiotemporal distribution of the mass concentration and OP of $PM_{2.5}$ measured by five different endpoints in the Midwest US.~~ The goal of this analysis is to compare the spatiotemporal distribution of $PM_{2.5}$ OP with that of the mass concentrations. We also want to investigate if different measures of OP, i.e. OP^{AA}, OP^{GSH}, $OP^{OH\text{-}SLF}$, OP^{DTT} and $OP^{OH\text{-}DTT}$ show different spatiotemporal trends or are correlated with each other. Correlations of OP with PM chemical composition and source apportionment analysis of $PM_{2.5}$ OP will be presented in our subsequent publications. Our paper presents the results from probably one of the most comprehensive OP analysis campaigns, combining five different acellular OP endpoints measured on both water- and organic-soluble extracts.

2 Experimental methods

2.1 Sampling campaign

Simultaneous sampling in five different sites spread across three states (i.e. Illinois, Indiana and Missouri) was conducted every week for this project in the Midwest US. The locations of the sampling sites are shown in Figure 1. Champaign (CMP) and Bondville (BON) sites are paired sites representing the urban (roadside) and rural environment of Champaign County, IL, respectively; while three major city sites [i.e. Chicago (CHI), Indianapolis (IND) and St. Louis (STL)] are representatives of urban background regions of ~~Chicago, Indianapolis and St. Louis, respectively~~these respective cities.

CMP is located on a parking garage in the campus of University of Illinois at Urbana-Champaign, and is adjacent to a 2-lane (both ways) road (i.e. University Avenue). This site is surrounded by the university facilities and is impacted by traffic emissions from adjacent road. The site is about 1 km from downtown Champaign and is surrounded by dense housing and business development.

BON is a rural site, 15 km west of downtown Champaign, and is also a part of the IMPROVE (Interagency Monitoring of Protected Visual Environments) monitoring program. The station is managed by the Illinois State Water Survey, and is surrounded by intensively managed agricultural fields. The major highways (I-57 and I-74) are at least 6 km north and east of this site, respectively.

CHI site is located on a dormitory building – Carman hall in Illinois Institute of Technology (IIT) campus, Chicago, IL. This site is ~500 m away from a two-way 6-lane (including an emergency lane) interstate highway I-90/94, 1.5 km west of Lake Michigan and 5 km south of downtown Chicago. The highway I-90/94 has an annual average daily traffic flow of 300,000 vehicles per day, and heavy-duty vehicles account for ~10% in the traffic fleet (Xiang et al., 2019). The site is situated in the mixed commercial and residential area of Chicago, and therefore the emissions from both traffic mixed with residential and commercial activities are expected.

IND site is located inside the campus of School of Public Health, Indiana University – Purdue University Indianapolis (IUPUI). This site is close to downtown Indianapolis (2 km southeast of IND site) and a two-way 4-lane interstate highway I-65 (1 km northeast of IND site). The site is surrounded by miscellaneous facilities of IUPUI and Riley Hospital, therefore the sources of ambient aerosols at IND site may include vehicular emissions from highway, and emissions from residential and commercial activities related to miscellaneous university and hospital operations.

STL site is located 3 km north of downtown St. Louis, MO. This site is 230 m west of the interstate I-44/70 and 1.2 km west of Mississipi River. It is also surrounded by several industries for steel processing, zinc smelting and copper production (Lee et al., 2006). Therefore, a significant portion of metals in PM at this site is supposed to be from industrial emissions. The urban activities in downtown St. Louis as well as traffic emissions from highway vehicles and river boating are also potential sources of $PM_{2.5}$ at this site.

The sampling period involved four seasons starting from May 22, 2018 to May 30, 2019. Integrated ambient $PM_{2.5}$ samples were collected simultaneously for three continuous days from all the sites. Each site was instrumented with

a High-volume (Hi-Vol) air sampler equipped with $PM_{2.5}$ inlet (flow rate = 1.13 m^3/min; Tisch Environmental; Cleves, OH). Both before and after the sampling campaign, we did a comparison of various samplers by running them in parallel to collect $PM_{2.5}$ samples and analyzing them for OP^{DTT} (see Section S1 of the supplemental information, SI). All the samplers were equipped with a timer to enable automatic start of the sampling on each Tuesday 0:00, and turn-off on each Friday 0:00. After the sampled filters were collected on Friday (before noon), new filters were loaded in the filter holder to start next run of sampling. All five samplers were monthly calibrated for the flow rate by using a variable flow calibration kit (Tisch Environmental), and the flow rate was measured every week before and after the sampling. We used quartz filters (Pall TissuquartzTM, 8"×10") for collecting $PM_{2.5}$. The filters were prebaked at 550 °C for 24 hours before sampling. Total 241 filters were collected during the whole campaign (44 from CHI, 47 from STL, 54 from IND, 51 from CMP and 45 from BON). We also collected field blank filters (N = 10 from each site) once in every five weeks by placing a blank quartz filter in filter holder of the sampler for 1 hour but without running the pump.

All filters were weighed before and after sampling using a lab-scale digital balance (0.2 mg readability, Sartorius A120S, Götingen, Germany) for determining the $PM_{2.5}$ mass loading on each filter. Prior to each weighing, filters were equilibrated in a constant temperature (24 °C) and relative humidity (50 %) room for 24 hours. After sampling, the filters were individually wrapped in prebaked (550 °C) aluminum foils and stored in a freezer at -20 °C before analysis. More information on sampling including the exact dates of sampling are provided in Table S1 in the supplemental information (SI).

2.2 Sample extraction protocol

Sample extraction protocol for OP analysis was determined by the requirement to keep a relatively constant concentration of $PM_{2.5}$ in the liquid extracts. This is due to non-linear response of certain OP endpoints with $PM_{2.5}$ mass in the extracts (Charrier et al., 2016). Thus, fraction of the filter and the volume of water used for extraction were varied depending on the $PM_{2.5}$ mass loading on each Hi-Vol filter. For the analyses of water-soluble OP, a few (usually 3-5) circular sections (16-25 mm diameter) were punched from the filter and immersed into 15-20 mL of deionized Milli-Q water (DI, resistivity = 18.2 MΩ/cm). The volume of water was adjusted to achieve ~100 µg of total $PM_{2.5}$ per mL of DI. The vials containing filter sections suspended in the DI were sonicated in an ultrasonic water bath for 1 hour (Cole-Palmer, Vernon-Hills, IL, US). These suspensions were then filtered through a 0.45 µm PTFE syringe filter to remove all water-insoluble components including filter fibers. 10.5 mL of these filtered extracts were separated and diluted with DI to 15 mL. These diluted extracts were then kept in the sample queue of SAMERA for OP analyses. SAMERA withdraws different volume of these extracts into the reaction vials (RVs) for each OP measurement, i.e. 3.5 mL for OP^{AA}, OP^{GSH} and $OP^{OH\text{-}SLF}$, and 2.1 mL for OP^{DTT} and $OP^{OH\text{-}DTT}$ measurements, all of which were further diluted to 5 mL in the RVs. Thus, the concentrations of $PM_{2.5}$ in RVs for SLF-based (i.e. OP^{AA}, OP^{GSH} and $OP^{OH\text{-}SLF}$) and DTT-based (i.e. OP^{DTT} and $OP^{OH\text{-}DTT}$) assays were maintained constant at 50 µg/mL and 30 µg/mL (±1%), respectively.

For methanol-soluble OP measurements, another fraction from each filter having the same area as used for the water-soluble $PM_{2.5}$ extraction was punched and extracted in 10 mL of methanol. After sonication for 1 hour, the suspensions were filtered through 0.45 μm PTFE syringe filter. The filtered extracts were then concentrated to less than 50 μL using a nitrogen dryer to evaporate methanol, and were subsequently reconstituted in~~to 15-20 mL of~~ DI to the exact same volume as the water-soluble extracts. Reconstituted methanol extracts were vigorously shaken on an analog vortex mixer (VWR International, Batavia, IL, US) for at least 60 seconds at 3200 rpm to ensure a thorough flushing of the components probably deposited along the wall of the vials during evaporation. These methanol-soluble extracts were then~~and~~ analyzed for OP in the same way as water-soluble extracts.

2.3 OP analysis

OP activities of $PM_{2.5}$ extracts were analyzed using SAMERA. The setup and operation protocol of SAMERA has been discussed in detail in Yu et al. (2020). Briefly, the analysis of all OP endpoints for each extract was conducted in two stages: SLF-based endpoints were analyzed first, while DTT-based assays were conducted in the second stage. For measuring OP^{AA} and OP^{GSH}, 3.5 mL of the extract was mixed with 0.5 mL SLF and 1 mL of 0.5 M potassium phosphate buffer (K-PB) in an RV. SLF was made following the protocol of Yu et al. (2020), i.e. by mixing equal volumes (1 mL each) of four antioxidant stock solutions – 20 mM AA, 10 mM GSH, 30 mM citric acid (CA) and 10 mM UA, and diluting the mixture by DI to 10 mL. Final concentrations of the antioxidants in the RV used for incubating the sample, were 200 μM AA, 100 μM GSH, 300 μM CA and 100 μM UA. At certain time intervals (i.e. 5, 24, 43, 62 and 81 minutes), two small aliquots of the reaction mixture were withdrawn and dispensed into two measurement vials (MV1 and MV2) separately. The mixture in MV1 was diluted by DI, and was directly injected into a liquid waveguide capillary cell (LWCC-3100; World Precision Instruments, Inc., Sarasota, FL, USA) coupled to an online spectrophotometer (Ocean Optics, Inc., Dunedin, FL, USA), which measured the absorbance at 265 nm (signal from AA) and 600 nm (background) for determining the concentration of AA. 1.6 mL of o-phthalaldehyde (OPA) was added into the reaction mixture contained in MV2 to react with GSH, which forms a fluorescent product. The final mixture in MV2 was then pushed through a flow cell equipped in a Horiba Fluoromax-4 spectrofluorometer (Horiba Scientific, Edison, NJ, USA), and the fluorescence was measured at excitation/emission wavelength of 310 nm/427 nm. Simultaneously with the preparation of the reaction mixture for OP^{AA} and OP^{GSH} analyses, 3.5 mL of the extract was mixed with 0.5 mL SLF and 1 mL of 50 mM K-PB buffered disodium terephthalate (TPT) (pH = 7.4) in another RV2. TPT captures ·OH generated in the reaction and forms another fluorescent product 2-hydroxyterephthalic acid (2-OHTA). Small aliquots of this reaction mixture were withdrawn into MV2 at selected time intervals (10, 29, 48, 67 and 86 minutes), diluted by DI, and injected into the flow cell of the spectrofluorometer for measuring fluorescence at the same wavelengths as used for GSH measurement (i.e. 310 nm excitation/427 nm emission). The concentration of 2-OHTA was determined by calibrating various concentrations (10-500 nM) of 2-OHTA standards, and the generation rate of ·OH was determined as the formation rate of 2-OHTA divided by a yield factor (0.35) (Son et al., 2015).

Both RVs and MVs were flushed with DI after all SLF-based endpoints were analyzed, and DTT-based assays started immediately after this cleaning. Similar to the first step of SLF assay, 2.1 mL of the diluted $PM_{2.5}$ extract was mixed

with 1 mL of 50 mM TPT, 1.4 mL of DI and 0.5 mL of 1 mM DTT in an RV. At certain time intervals (i.e. 5 min, 17 min, 29 min, 41 min and 53 min), two small aliquots of this reaction mixture were withdrawn and diluted with DI in MV1 and MV2 separately for the measurement of DTT and ·OH, respectively. DTNB was added into MV1 to capture residual DTT. The final mixture in MV1 was pushed through LWCC to measure the absorbance at 412 nm, while the mixture in MV2 was pushed through flow cell of the spectrofluorometer for fluorescence measurement (310 nm excitation/427 nm emission), respectively. The system was again cleaned by flushing DI to RVs, MVs, LWCC and flow cell of the spectrofluorometer for the next run. Once in a week, we conducted thorough cleaning of the entire system, by replacing all chemicals and samples first with methanol followed by DI, and running the program script 10 times with each solvent.

2.4 Quality Control/Quality Assurance

One field blank filter extract along with a DI blank were used as the negative controls for each set of $PM_{2.5}$ samples analyzed in a batch (usually ~10). Selected metals and organic compounds that are known to be sensitive for different OP endpoints, i.e. Cu(II) for OP^{AA} and OP^{GSH}, Fe(II) for $OP^{OH\text{-}SLF}$, phenanthraquinone (PQ) for OP^{DTT} and 5-hydroxy-1,4-naphthoquinone (5-H-1,4-NQ) for $OP^{OH\text{-}DTT}$, were used as the positive control, and were analyzed weekly with $PM_{2.5}$ samples to ensure the stability of SAMERA and correct for any possible drift.

The average and standard deviation of OP of negative and positive controls are shown in Table 1. Our previous study on the development of SAMERA (Yu et al., 2020) reported the values of OP for negative controls, as 0.17 ± 0.07 μM/min for OP^{AA}, 0.37 ± 0.06 μM/min for OP^{GSH}, 4.57 ± 1.21 nM/min for $OP^{OH\text{-}SLF}$, 0.65 ± 0.02 μM/min for OP^{DTT} and -0.38 ± 0.24 μM/min for $OP^{OH\text{-}DTT}$, which are consistent with the values reported in Table 1. The precision of SAMERA was assessed previously using water-soluble extracts and the coefficient of variations (CoVs) were reported to be less than 14 % (7.9 – 13.3 %) for all OP endpoints (Yu et al., 2020). We also assessed the precision using methanol-soluble extracts and found similar levels of CoVs, i.e. 8.9 -14.5 % for all OP endpoints (see Table S2 in SI). Consistency of our current results for negative controls with those reported earlier, and ~~a~~ the low ~~coefficient of variation (~~CoVs~~)~~ obtained for the positive controls (1.1 – 11.8%) and $PM_{2.5}$ extracts ensured a good quality assurance for the overall OP analysis. We blank corrected all OP values of ambient samples by subtracting the averaged field blank measurements. After blank correction, the OP values below detection limit were replaced with half of the detection limits for the corresponding OP endpoint. The mass-normalized (intrinsic, OPm) and volume-normalized (extrinsic, OPv) OP levels were obtained by dividing the blank corrected OP activities by the extracted $PM_{2.5}$ mass (for OPm) and by the volume of air collected on the extracted fractions of filters (for OPv), respectively. The detailed calculations of OPm and OPv have been previously described in Yu et al. (2020).

2.5 Statistical analysis

To assess spatiotemporal variability in both OP and $PM_{2.5}$ mass, we compared their differences among all sites and seasons using one-way analysis of variance (ANOVA) test, and different pairs (i.e. pairs of different sites or seasons) were compared by Fisher's least significant difference (LSD) post-hoc test. The significant and highly significant differences were considered by one-way ANOVA when $P < 0.05$ and $P < 0.01$, respectively. Pearson's correlation

coefficient (r) for single linear regression was computed to determine the correlation of OP between different sites, between water-soluble and methanol-soluble OP, between OP and $PM_{2.5}$, as well as the intercorrelation among different endpoints for each site. All $PM_{2.5}$ samples were assessed for spatiotemporal variability. However, ~~Since~~ since several OP endpoints (e.g. OP^{AA}, OP^{GSH} and OP^{DTT}) were abnormally elevated in the week of July 4th (Independence Day celebration; discussed in section 3.2), we removed this week's sample from our regression analysis to avoid any bias caused by this episodic event. Site-to-site comparisons were performed by calculating the coefficient of divergence (COD) of mass concentration and volume-normalized OP (i.e. OPv) for all site pairs, as follows:

$$CoD = \sqrt{\frac{1}{N}\sum_{i=1}^{N}\left(\frac{c_{ij} - c_{ik}}{c_{ij} + c_{ik}}\right)^2}$$

where: c_{ij} and c_{ik} are the $PM_{2.5}$ mass or OPv measured in the same week *i* at sites *j* and *k*, respectively; N is the number of the comparable sample pairs for sites *j* and *k*. COD ranges from 0 to 1. A larger COD (closer to 1) indicates more spatial heterogeneity between the sites, while a smaller COD (closer to 0) implies spatial homogeneity. One-way ANOVA test was conducted in Matlab R2019a, while other statistical analyses were carried out using Excel.

3 Results and Discussion

3.1 $PM_{2.5}$ mass concentration

Figure 2 shows the time series of three-days averaged $PM_{2.5}$ mass concentration at five sampling sites, while the seasonal averages are shown in Table 2. The mass concentrations ranged from 2.0 to 21.7 μg/m^3 across all sites, and the median was 11.0 μg/m^3. These results are comparable with ~~previous studies on~~the typical ranges of $PM_{2.5}$ in Midwest US cities (2.1 – 48.6 μg/m^3), e.g. St. Louis ~~(3.9 - 48.6 μg/m^3)~~ (Lee et al., 2006), Chicago ~~(median 9.4 – 10.7 μg/m^3)~~ (Milando et al., 2016), Detroit ~~(0.6 – 56.2 μg/m^3, median 14.4 – 17.6 μg/m^3)~~ (Gildemeister et al., 2007), Bondville ~~(2.1 – 36.5 μg/m^3, median 9.5 μg/m^3)~~ and selected cities in Iowa (e.g. Cedar Rapids, Des Moines and Davenport) ~~(8.4 – 11.6 μg/m^3)~~ (Kundu and Stone, 2014), as measured in several previous studies. Generally, the more urbanized sites of our study (i.e. CHI, STL and IND) showed slightly higher mass concentrations (5.7 – 21.7 μg/m^3; median: 11.8 μg/m^3) compared to the smaller cities like CMP and its rural component (i.e. BON) (2.0 – 20.2 μg/m^3; median: 9.2 μg/m^3). The highest mass concentrations were recorded at CHI ~~(~~during winter ($P < 0.01$; Table S3) and STL ~~(~~during summer ($P < 0.05$), while BON exhibited the lowest concentrations in all seasons, except fall when the mass concentrations were lowest at CMP ($P < 0.05$). Other than these minor variations, the $PM_{2.5}$ mass concentrations are both spatially and temporally homogeneous in the Midwest US with no significant seasonal differences ($P > 0.05$ at most sites).

3.2 ~~Time series~~Spatiotemporal variation in ~~of~~ $PM_{2.5}$ OP

Time series of both mass- and volume-normalized OP (OPm and OPv, respectively) at all the sites are shown in Figure 3 (water-soluble OP) and Figure 4 (methanol-soluble OP). Seasonally averaged OPm and OPv of water-soluble and

methanol-soluble $PM_{2.5}$ are also shown in Figures 5 and 6, respectively. Differences in both OPm and OPv among different seasons or sites were determined by one-way ANOVA and the results are listed in SI, Table S4 (water-soluble OP) and Table S5 (methanol-soluble OP). Generally, OP ~~for both water- and methanol-soluble extracts~~ showed much more spatiotemporal variability than the $PM_{2.5}$ mass in the Midwest US.

Water-soluble $PM_{2.5}$ OP

~~The~~ Figures 3 and 5 (time series and seasonal averages of water-soluble OP) showed a significant spatial variability for SLF-based endpoints, particularly ~~(i.e.~~ OP^{AA}~~,~~ and OP^{GSH}, ~~and $OP^{OH\text{-}SLF}$)~~in comparison to DTT-based OP (i.e. OP^{DTT} and $OP^{OH\text{-}DTT}$) ~~in~~ for both mass- and volume-normalized results ~~(Figure 3a-c)~~. Highest OP^{AA} and OP^{GSH} activities (both mass- and volume-normalized) occurred at ~~the roadside site~~ CMP (~~as confirmed by 1-way ANOVA test;~~ $P < 0.01$) in most seasons ~~(except winter for OP^{AA}v), while STL and IND had the lowest OP^{AA} and OP^{GSH}~~. $OP^{OH\text{-}SLF}$ was more spatially uniformly distributed than OP^{AA} and OP^{GSH}; significantly higher $OP^{OH\text{-}SLF}$m and $OP^{OH\text{-}SLF}$v were observed at CMP only in summer and spring ($P < 0.05$). For the DTT-based endpoints, OP^{DTT}v was only marginally higher at CHI in winter, and at CMP in summer and spring. Other than that, no significant differences were observed for OP^{DTT}v among various sites. The spatially uniform pattern for OP^{DTT}v is consistent with Verma et al. (2014) which found limited spatial variation for OP^{DTT}v in the Southeast US. In contrast, there was a significant variation in the OP^{DTT}m with elevated levels at CMP ($P < 0.01$) in all seasons. Interestingly, the $OP^{OH\text{-}DTT}$ endpoint showed more spatial variability and was generally lowest at CMP ($P < 0.05$) – the site which showed highest levels for ~~all~~ other OP endpoints. It implies that although OP^{DTT} and $OP^{OH\text{-}DTT}$ endpoints are measured in the same DTT assay, different chemical components play differential roles in these endpoints. We found very similar spatial patterns of mass- and volume-normalized OP activities for most endpoints, ~~again~~ indicating only a marginal role of $PM_{2.5}$ mass concentrations in causing the spatial variability in OP levels.

~~Differences in both OPm and OPv among different seasons or sites were determined by one-way ANOVA and the results are listed in SI, Table S4.~~ Seasonally, highest OP activities were generally observed in summer, while the lowest activities usually occurred in winter (Figure 5). ~~For example, OP^{AA}v and OP^{GSH}v activities had highest levels in summer and lowest levels in winter at CMP and BON, as verified by 1-way ANOVA ($P < 0.05$). Similarly, significantly higher OP activities ($P < 0.01$ for most cases) were observed for both $OP^{OH\text{-}SLF}$m and $OP^{OH\text{-}SLF}$v at all five sites in summer, while winter showed significantly lower levels ($P < 0.05$). For DTT-based endpoints, $OP^{OH\text{-}DTT}$m and $OP^{OH\text{-}DTT}$v also showed higher values in summer at CHI, IND and CMP ($P < 0.01$). However, OP^{DTT} exhibited limited temporal variation at most sites with only slightly higher OP^{DTT}m and OP^{DTT}v observed in summer at BON ($P < 0.05$).~~ An exception to this trend was OP^{DTT}, which exhibited limited temporal variation at most sites with only slightly higher OP^{DTT} observed in summer at BON ($P < 0.05$). The temporal ~~variation trend~~uniformity of OP^{DTT} in this study does not correspond with previous studies conducted in Southwest and Southeast US. For the Southeast US, Verma et al. (2014) found significantly higher OP^{DTT}v in winter (December, 2012) compared to summer (June to August, 2012), and this difference was even more pronounced in mass-normalized OP. Saffari et al. (2014) also observed higher OP^{DTT} activities of quasi-ultrafine particles ($PM_{0.25}$) in fall and winter seasons for the Southwest US (Los Angeles Basin), and attributed this trend to the partitioning of redox-active semi-volatile organic compounds to

particle phase in colder seasons. However, the trend of OP^{AA} in our study is in agreement with another study in Southeast US ~~using OP^{AA} as the endpoint~~ (Fang et al., 2016), which showed higher OP^{AA} in warmer seasons (i.e. summer and fall) than winter. ~~There is no previous literature available on the spatiotemporal trends of other OP endpoints in US, to which we can compare our results.~~The seasonal trend of mass- and volume-normalized activities were nearly identical for all endpoints, again indicating a marginal effect of $PM_{2.5}$ mass concentration in the temporal variation of OP.

~~CMP showed a substantially higher water-soluble OP than other sites for these endpoints. In the temporal trend, SLF-based endpoints showed higher levels during summer compared to other seasons at most sites.~~ A significant temporal variation was observed for CMP with several spikes in the OP activities throughout the year, most prominently for OP^{AA} (Figure 3). These spikes might be attributed to the traffic, as CMP is the only site adjacent (< 10 m) to a major urban road and located on the roof of a parking garage. One of our previous studies, Wang et al. (2018), reported large variations in several redox-active metals (e.g. Cu, Fe, Mn, Pb and Zn), which have been known to be related with the vehicular emissions (Hulskotte et al., 2007;Garg et al., 2000;Gietl et al., 2010;Apeagyei et al., 2011;Councell et al., 2004), at the same CMP site. Since SLF-based endpoints have been shown to be highly sensitive towards metals (Ayres et al., 2008;Calas et al., 2018;Fang et al., 2016;Moreno et al., 2017;Charrier and Anastasio, 2015;Wei et al., 2018), the temporal variation in traffic intensity probably contributes to the spikes observed at CMP. The peaks in the week of July 3 were observed for multiple endpoints (e.g. OP^{AA}, OP^{GSH} and OP^{DTT}) at most sites, which is attributed to the emissions from firecrackers on Independence Day (July 4) celebrations (Yu et al., 2020;Puthussery et al., 2018).

Methanol-soluble $PM_{2.5}$ OP

~~As observed in the time series, the spatiotemporal variations for the methanol-soluble OP endpoints (e.g. OP^{AA}, OP^{GSH}, OP^{DTT} and $OP^{OH\text{-}DTT}$) seem to be lesser than the corresponding water-soluble OP (Figure 4a-b, d-e). However, methanol-soluble $OP^{OH\text{-}SLF}$ showed a significant seasonal variability with substantially higher levels in summer at most sites, and a marginal spatial variability with slightly higher activities at CHI during summer (Figure 4c).~~

~~Seasonal averages of methanol-soluble $PM_{2.5}$ OPm and OPv are shown in Figure 6.~~ Compared to water-soluble OP, most OP endpoints in the methanol-soluble extracts showed weaker seasonal variations (Figure 4 and 6), as also ~~indicated~~ confirmed by relatively lower F-values [median of F = 1.61 (Table S5a), compared to 2.71 for the water-soluble OP endpoints (Table S4a)]. Similar to water-soluble OP, highest activities for the methanol-soluble OP were generally observed in summer (Figure 6). ~~For example, highest values of OP^{AA} and OP^{DTT} were observed in summer at CMP and BON ($P < 0.05$) for both mass- and volume-normalized activities. $OP^{OH\text{-}SLF}$m and $OP^{OH\text{-}SLF}$v peaked in summer at BON ($P < 0.01$), but in fall at IND ($P < 0.05$). $OP^{OH\text{-}DTT}$m and $OP^{OH\text{-}DTT}$v were also elevated in summer at CHI ($P < 0.01$), but showed marginal seasonal variations at other sites. In contrast, OP^{GSH} showed a rather homogeneous seasonal distribution at all sites, except slight elevation of OP^{GSH}m in fall at STL and IND ($P < 0.05$).~~ The spatial variations in OP were also weaker for the methanol-soluble extracts in comparison to water-soluble extracts [median of F = 1.96 (Table S5b), compared to 4.52 for the water-soluble OP endpoints (Table S4b~~)];~~)]. ~~h~~However, some ~~spikes~~ significantly higher OP levels were observed at certain sites in different seasons, e.g. OP^{AA}v at CHI in winter and spring, OP^{GSH}v at CHI and CMP during winter and spring, OP^{GSH}m at CMP in all seasons, $OP^{OH\text{-}}$

^{SLF} at CHI in summer and winter, and $OP^{OH\text{-}DTT}m$ and $OP^{OH\text{-}DTT}v$ at CHI in summer ($P < 0.05$). ~~Substantially higher $OP^{AA}v$ occurred at CHI ($P < 0.05$) in winter and spring, while no significant differences were observed for $OP^{AA}m$ among different sites in any other season. $OP^{GSH}v$ was elevated at CHI and CMP during winter and spring ($P < 0.05$), while CMP showed elevated $OP^{GSH}m$ in all seasons ($P < 0.05$). In summer and winter, $OP^{OH\text{-}SLF}$ peaked at CHI ($P < 0.05$) for both mass- and volume-normalized levels. $OP^{OH\text{-}DTT}m$ and $OP^{OH\text{-}DTT}v$ also peaked at CHI ($P < 0.05$) in summer. The lowest levels of $OP^{OH\text{-}DTT}$ were again found at CMP in all seasons, which is consistent with the trend for water soluble $OP^{OH\text{-}DTT}$. In contrast, OP^{DTT} showed spatially homogeneous distribution across all seasons, with marginally elevated values of $OP^{DTT}v$ at STL during fall and winter ($P < 0.05$).~~ Other than these few cases, ~~T~~the spatiotemporal trends were again ~~very~~ largely similar between mass- and volume-normalized methanol-soluble OP activities ~~except few cases discussed here~~.

Comparison of OP in the Midwest US with previous investigations

A comparison of the ranges of OP endpoints ~~observed~~ measured in our study ~~and~~ with those reported in previous ~~investigations~~ studies is ~~has been briefly~~ provided in ~~SI (~~Table S6~~2~~ (SI). The purpose of this comparison is to validate our measurements and present a larger perspective on the general levels of OP in the Midwest US in comparison to other regions of the world. For water-soluble $PM_{2.5}$ in our study, $OP^{AA}m$ ranged from 0.002 to 0.077 nmol·min^{-1}·μg^{-1}, which is within the ranges reported from previous studies conducted in Europe (Künzli et al., 2006;Szigeti et al., 2016;Godri et al., 2011;Perrone et al., 2019) and India (Mudway et al., 2005). ~~However, our~~Our range of $OP^{AA}v$ (0.012 – 0.908 nmol·min^{-1}·m^{-3}) is comparable with Gao et al. (2020a) (0.023 – 0.126 nmol·min^{-1}·m^{-3}), but is much lower than that reported by Fang et al. (2016) (0.2 – 5.2 nmol·min^{-1}·m^{-3}) and Yang et al. (2014) (0.8 – 35.0 nmol·s^{-1}·m^{-3}), probably because of a different protocol used in those ~~their~~ studies~~y~~, both of which involved only AA in the assay. The median of water-soluble $OP^{GSH}m$ (0.007 nmol·min^{-1}·μg^{-1}) is also comparable with the average of those reported (0.0041 – 0.0083 nmol·min^{-1}·μg^{-1}) in previous studies (Mudway et al., 2005;Künzli et al., 2006;Godri et al., 2011). Similarly, the median of $OP^{OH\text{-}SLF}m$ (0.142 pmol·min^{-1}·μg^{-1}) is comparable to the averages reported by Vidrio et al. (2009) ~~(0.253 pmol·min^{-1}·μg^{-1})~~ and Ma et al. (2015) (0.092 – 0.253 pmol·min^{-1}·μg^{-1}). The median of $OP^{DTT}m$ (0.014 nmol·min^{-1}·μg^{-1}) of our samples is significantly lower than the medians or averages reported from most studies conducted in US ~~(0.019 – 0.041 nmol·min^{-1}·μg^{-1})~~ (Cho et al., 2005;Charrier and Anastasio, 2012;Gao et al., 2020b;Hu et al., 2008;Fang et al., 2015) and Greece (0.019 – 0.041 nmol·min^{-1}·μg^{-1}) (Paraskevopoulou et al., 2019), but is closer to the averages reported from the studies conducted in Italy (0.010 – 0.012 nmol·min^{-1}·μg^{-1}) (Cesari et al., 2019;Perrone et al., 2019). Similarly, the median of our $OP^{DTT}v$ (0.150 nmol·min^{-1}·m^{-3}) is lower compared to several studies in Southeast US and Europe (0.19 – ~~0.31~~0.33 nmol·min^{-1}·m^{-3}) (Fang et al., 2015;Gao et al., 2017;Gao et al., 2020a;Gao et al., 2020b;Paraskevopoulou et al., 2019;Perrone et al., 2019;Cesari et al., 2019), but closer to one study conducted in Southwest US (0.14 nmol·min^{-1}·m^{-3}) (Hu et al., 2008). The range of water-soluble $OP^{OH\text{-}DTT}v$ of our samples is quite large (0.004 – 3.565 pmol·min^{-1}·m^{-3}); however, there is no previous data to compare it, other than reported in the studies conducted by our own group (Xiong et al., 2017;Yu et al., 2018), which were based on a much smaller sample size (N = 10) and limited spatial extent (single site) and thus resulting in~~to~~ a much narrower range (0.2 – 1.1 pmol·min^{-1}·m^{-3}). Compared to water, only a handful of studies on ~~PM~~ OP^{AA} and OP^{DTT} have used methanol as the PM extraction

solvent, while no previous literatures have investigated is available on the OP of methanol-soluble PM for other endpoints. Similar to the water-soluble OP results, the level of methanol-soluble $OP^{AA}v$ in our study (0.030 – 0.311 nmol·min^{-1}·m^{-3}) was lower than that reported by Yang et al. (2014) (2.2 – 43.5 nmol·s^{-1}·m^{-3}), probably due to different measurement protocols (only AA in comparison to SLF in our approach). The medians of our methanol-soluble $OP^{DTT}m$ (0.021 nmol·min^{-1}·μg^{-1}) and $OP^{DTT}v$ (0.234 nmol·min^{-1}·m^{-3}) are slightly lower than the medians or averages reported in previous studies in the Southeast US (0.027 – 0.034 nmol·min^{-1}·μg^{-1} and 0.28 – 0.30 nmol·min^{-1}·m^{-3}, respectively for $OP^{DTT}m$ and $OP^{DTT}v$) (Verma et al., 2012;Gao et al., 2017;Gao et al., 2020b), which is consistent with the trend for water-soluble OP^{DTT} (i.e. lower levels of our samples than reported previously at other sites).

3.3 Spatiotemporal variation in $PM_{2.5}$ OP

Water-soluble $PM_{2.5}$ OP

CMP showed a substantially higher water-soluble OP than other sites for these endpoints. In the temporal trend, SLF-based endpoints showed higher levels during summer compared to other seasons at most sites. A significant temporal variation was observed for CMP with several spikes in the OP activities throughout the year, most prominently for OP^{AA}. The peak in the week of July 3 were observed for multiple endpoints (e.g. OP^{AA}, OP^{GSH} and OP^{DTT}) at most sites, which is attributed to the emissions from firecrackers on Independence Day (July 4) celebrations . In comparison to SLF-based endpoints, mass- and volume-normalized DTT-based OP (i.e. OP^{DTT} and $OP^{OH\text{-}DTT}$) showed lesser spatial variations (Figure 3d-e).Seasonally averaged OPm and OPv of water-soluble $PM_{2.5}$ at different sites are shown in Figure 5. Differences in both OPm and OPv among different seasons or sites were determined by one-way ANOVA and the results are listed in SI, Table S3. Seasonally, highest OP activities were generally observed in summer, while the lowest activities usually occurred in winter. For example, $OP^{AA}v$ and $OP^{GSH}v$ activities had highest levels in summer and lowest levels in winter at CMP and BON, as verified by 1-way ANOVA ($P < 0.05$). Similarly, significantly higher OP activities ($P < 0.01$ for most cases) were observed for both $OP^{OH\text{-}SLF}m$ and $OP^{OH\text{-}SLF}v$ at all five sites in summer, while winter showed significantly lower levels ($P < 0.05$). For DTT based endpoints, $OP^{OH\text{-}DTT}m$ and $OP^{OH\text{-}DTT}v$ also showed higher values in summer at CHI, IND and CMP ($P < 0.01$). However, OP^{DTT} exhibited limited temporal variation at most sites with only slightly higher $OP^{DTT}m$ and $OP^{DTT}v$ observed in summer at BON ($P < 0.05$). The seasonal trend of mass- and volume-normalized activities were nearly identical for all endpoints, indicating a marginal effect of $PM_{2.5}$ mass concentration in the temporal variation of OP.

The temporal variation trend of OP^{DTT} in this study does not correspond with previous studies conducted in Southwest and Southeast US. For the Southeast US, Verma et al. (2014) found significantly higher $OP^{DTT}v$ in winter (December, 2012) compared to summer (June to August, 2012), and this difference was even more pronounced in mass-normalized OP. Saffari et al. (2014) also observed higher OP^{DTT} activities of quasi-ultrafine particles ($PM_{0.25}$) in fall and winter seasons for the Southwest US (Los Angeles Basin), and attributed this trend to the partitioning of redox-active semi-volatile organic compounds to particle phase in colder seasons. However, the trend of OP^{AA} in our study is in agreement with another study in Southeast US using OP^{AA} as the endpoint (Fang et al., 2016), which showed higher

~~OP^{AA} in warmer seasons (i.e. summer and fall) than winter. There is no previous literature available on the spatiotemporal trends of other OP endpoints in US, to which we can compare our results.~~

~~Spatially, there seems higher variability in the SLF based endpoints, i.e. OP^{AA} and OP^{GSH} than the DTT based endpoints (OP^{DTT} and $OP^{OH\text{-}DTT}$). Highest OP^{AA} and OP^{GSH} activities (both mass- and volume-normalized) occurred at the roadside site CMP (as confirmed by 1-way ANOVA test; $P < 0.01$) in most seasons (except winter for $OP^{AA}v$), while STL and IND had the lowest OP^{AA} and OP^{GSH}. $OP^{OH\text{-}SLF}$ was more spatially uniformly distributed than OP^{AA} and OP^{GSH}; significantly higher $OP^{OH\text{-}SLF}m$ and $OP^{OH\text{-}SLF}v$ were observed at CMP only in summer and spring ($P < 0.05$). For the DTT based endpoints, $OP^{DTT}v$ was only marginally higher at CHI in winter, and at CMP in summer and spring. Other than that, no significant differences were observed for $OP^{DTT}v$ among various sites. The spatially uniform pattern for $OP^{DTT}v$ is consistent with Verma et al. (2014) which found limited spatial variation for $OP^{DTT}v$ in the Southeast US. In contrast, there was significant variation in the $OP^{DTT}m$ with elevated levels at CMP ($P < 0.01$) in all seasons. Interestingly, the $OP^{OH\text{-}DTT}$ endpoint showed more spatial variability and was generally lowest at CMP ($P < 0.05$) – the site which showed highest levels for all other OP endpoints. It implies that although OP^{DTT} and $OP^{OH\text{-}DTT}$ endpoints are measured in the same DTT assay, different chemical components play differential roles in these endpoints. We found very similar spatial patterns of mass- and volume-normalized OP activities for most endpoints, again indicating only a marginal role of $PM_{2.5}$ mass concentrations in causing the spatial variability in OP levels.~~

~~*Methanol-soluble $PM_{2.5}$ OP*~~

~~The spatiotemporal variations for the methanol-soluble OP endpoints (e.g. OP^{AA}, OP^{GSH}, OP^{DTT} and $OP^{OH\text{-}DTT}$) seem to be lesser than the corresponding water-soluble OP (Figure 4a-b, d-e). However, methanol-soluble $OP^{OH\text{-}SLF}$ showed a significant seasonal variability with substantially higher levels in summer at most sites, and a marginal spatial variability with slightly higher activities at CHI during summer (Figure 4c).Seasonal averages of methanol-soluble $PM_{2.5}$ OPm and OPv are shown in Figure 6. Compared to water soluble OP, most OP endpoints in the methanol-soluble extracts showed weaker seasonal variations, as also indicated by relatively lower F-values [median of $F = 1.61$ (Table S4a), compared to 2.71 for the water-soluble OP endpoints (Table S3a)]. Similar to water-soluble OP, highest activities for the methanol-soluble OP were generally observed in summer. For example, highest values of OP^{AA} and OP^{DTT} were observed in summer at CMP and BON ($P < 0.05$) for both mass- and volume-normalized activities. $OP^{OH\text{-}SLF}m$ and $OP^{OH\text{-}SLF}v$ peaked in summer at BON ($P < 0.01$), but in fall at IND ($P < 0.05$). $OP^{OH\text{-}DTT}m$ and $OP^{OH\text{-}DTT}v$ were also elevated in summer at CHI ($P < 0.01$), but showed marginal seasonal variations at other sites. In contrast, OP^{GSH} showed a rather homogeneous seasonal distribution at all sites, except slight elevation of $OP^{GSH}m$ in fall at STL and IND ($P < 0.05$).~~

~~The spatial variations in OP were also weaker for the methanol-soluble extracts in comparison to water-soluble extracts [median of $F = 1.96$ (Table S4b), compared to 4.52 for the water-soluble OP endpoints (Table S3b)]; however, some spikes were observed at certain sites in different seasons. Substantially higher $OP^{AA}v$ occurred at CHI ($P < 0.05$) in winter and spring, while no significant differences were observed for $OP^{AA}m$ among different sites in any other season. $OP^{GSH}v$ was elevated at CHI and CMP during winter and spring ($P < 0.05$), while CMP showed elevated $OP^{GSH}m$ in all seasons ($P < 0.05$). In summer and winter, $OP^{OH\text{-}SLF}$ peaked at CHI ($P < 0.05$) for both mass- and~~

~~volume-normalized levels. $OP^{OH\text{-}DTT}$m and $OP^{OH\text{-}DTT}$v also peaked at CHI ($P < 0.05$) in summer. The lowest levels of $OP^{OH\text{-}DTT}$ were again found at CMP in all seasons, which is consistent with the trend for water-soluble $OP^{OH\text{-}DTT}$. In contrast, OP^{DTT} showed spatially homogeneous distribution across all seasons, with marginally elevated values of OP^{DTT}v at STL during fall and winter ($P < 0.05$). The spatiotemporal trends were again very similar between mass- and volume-normalized methanol-soluble OP activities except few cases discussed here.~~

3.~~4~~ 3 Comparison of water-soluble and methanol-soluble OP

To assess the effect of solvent on the OP response, we computed the ratio of methanol-soluble OPv to water-soluble OPv (M/W^{OP}) for all samples, and plotted it for the individual sites in Figure 7. As shown in the figure, methanol-soluble extracts generally showed greater response for most of the OP endpoints than the water-soluble extracts, with medians of M/W^{OP} being either close or greater than 1. The medians for M/W^{OP} for OP^{GSH}v and OP^{DTT}v were closer to 1 at many sites ~~(0.6 – 1.3 for OP^{GSH}v; and 1.1 – 1.9 for OP^{DTT}v)~~, while significantly greater than 1 for the other three endpoints (OP^{AA}v, $OP^{OH\text{-}SLF}$v and $OP^{OH\text{-}DTT}$v). The only exception to this trend was for OP^{AA}v at CMP, where significantly lower levels of methanol-soluble OP than water-soluble OP were observed (median of $M/W^{OP} = 0.7$ for OP^{AA}v at CMP). Our previous studies analyzing the chemical composition of PM collected at CMP have shown an elevated level of Cu (up to 60 ng/m^3) at this site (Wang et al., 2018;Puthussery et al., 2018), compared to the typical range (4 – 20 ng/m^3) at most urban sites in US (Buzcu-Guven et al., 2007;Kundu and Stone, 2014;Lee and Hopke, 2006;Hammond et al., 2008;Baumann et al., 2008;Milando et al., 2016). Although water-soluble Cu has been shown as the most important contributor to OP^{AA} (Fang et al., 2016;Ayres et al., 2008;Visentin et al., 2016), Lin and Yu (2020) reported a strong antagonistic interaction of Cu with imidazole and pyridine, both of which are alkaloid compounds (i.e. reduced organic nitrogen compounds), for oxidizing AA. The unprotonated nitrogen atom in alkaloids tends to chelate Cu, thus reducing its reactivity with AA. The antagonistic effect of Cu have been reported with other organic compounds (e.g. citric acid) as well (Pietrogrande et al., 2019). ~~Since many of the alkaloid compounds are water-insoluble but methanol-soluble, it is possible that these compounds are efficiently extracted in methanol, causing the~~ Thus, apparently lower levels of methanol-soluble OP^{AA} compared to the water-soluble OP^{AA} at CMP might be associated with the chelation of Cu by these alkaloids or other organic species, which could be more efficiently extracted in methanol.

The medians of M/W^{OP} were very high (1.4 – 3.8) for both ·OH based endpoints (i.e. $OP^{OH\text{-}SLF}$ and $OP^{OH\text{-}DTT}$v) ~~(2.1 – 3.8 for $OP^{OH\text{-}SLF}$v and 1.4 – 1.9 for $OP^{OH\text{-}DTT}$v)~~, indicating that methanol is able to more efficiently extract the redox-active components driving the response of these OP endpoints. In addition to ·OH-active organic species, e.g. quinones (Charrier and Anastasio, 2015;Xiong et al., 2017;Yu et al., 2018)~~We~~, which are more soluble in methanol, we suspect that one of such components could be organic-complexed Fe. As a Fenton reagent, Fe can catalyze the transfer of electrons from H_2O_2 to ·OH (Held et al., 1996). The generation of ·OH is further enhanced by the complexation of Fe with organic species (Wei et al., 2018;Gonzalez et al., 2017;Xiong et al., 2017;Yu et al., 2018). In a previous study conducted at our CMP site, Wei et al. (2018) found a significant fraction of Fe complexed with hydrophobic organic species (28 ± 22 %). That study also reported a substantially higher ratio of Fe concentration in 50 % methanol to that in water (1.42 ± 0.19), which showed some seasonality (1.97 ± 0.17 during winter and 1.33 ± 0.20 in summer). This

seasonal pattern of Fe solubility in methanol versus water is consistent with the time series of M/W^{OP} for $OP^{OH\text{-}SLF}v$ at most sites (showing higher values in winter than summer; SI Table S7~~5~~), which further corroborated that Fe complexed with hydrophobic organic fraction of $PM_{2.5}$ could be majorly responsible for the $OP^{OH\text{-}SLF}v$ and $OP^{OH\text{-}DTT}v$ in the methanol extracts. However, detailed chemical characterization will be needed to confirm these hypotheses, which will be explored in our subsequent publications.

We also calculated Pearson's r for the regression between respective water-soluble and methanol-soluble OP endpoints for individual sites, which are shown in Table 3. $OP^{DTT}v$ showed some good correlation between two extraction protocols (r = 0.43 – 0.74 except at STL), while correlations were generally poor (r < 0.60) for other four endpoints (i.e. $OP^{AA}v$, $OP^{GSH}v$, $OP^{OH\text{-}SLF}v$ and $OP^{OH\text{-}DTT}v$). It indicates that the components driving the response of OP^{DTT} could be more uniformly extracted in both water and methanol. However, there are additional water-insoluble species driving the response of $OP^{AA}v$, $OP^{GSH}v$, $OP^{OH\text{-}SLF}v$ and $OP^{OH\text{-}DTT}v$, which are more efficiently extracted in methanol than water.

3.~~5~~4 Site-to-site comparison of OP and mass concentration of $PM_{2.5}$

To further evaluate the spatial trend of OP across the Midwest US region, we calculated both COD and correlation coefficients (Pearson's r) for different site pairs, which are shown in Figure 8 (mass concentrations and water-soluble OP of $PM_{2.5}$), and Figure 9 (methanol-soluble $PM_{2.5}$ OP).

$PM_{2.5}$ mass concentration and water-soluble $PM_{2.5}$ OP

$PM_{2.5}$ mass concentrations showed low levels of CODs (0.13 – 0.25, median: 0.20), confirming a spatially homogeneous distribution of $PM_{2.5}$ as indicated earlier (Figure 8a). Conversely, we observed generally higher CODs (median = 0.27 – 0.43) for all water-soluble OPv endpoints~~, i.e. $OP^{AA}v$ (0.38 – 0.56, median: 0.43), $OP^{GSH}v$ (0.28 – 0.51, median: 0.35), $OP^{OH\text{-}SLF}v$ (0.30 – 0.40, median: 0.35), $OP^{DTT}v$ (0.19 – 0.34, median: 0.25), and $OP^{OH\text{-}DTT}v$ (0.21 – 0.38, median: 0.27)~~ (Figure 8b-f). Our results showing a stronger spatial variability in OP than PM mass are largely in agreement with a recent study (Daellenbach et al., 2020) analyzing a comprehensive dataset for OP in Europe, which showed that both OPv (measured by DTT, 2′,7′-Dichlorofluorescin Diacetate and AA assays) and PM_{10} mass concentrations were elevated in the urban environments (e.g. Paris and the Po valley), but PM_{10} was more regionally distributed than OPv.

Interestingly, we found poor correlations for $PM_{2.5}$ among all site pairs (r < 0.60), except IND and BON (r = 0.63). It implies that despite a homogeneous spatial distribution, emission sources of the chemical species composing $PM_{2.5}$ are different at different sites. The correlations were also weak (r < 0.60 for most cases) for the OP endpoints showing high CODs, i.e. OP^{AA}, OP^{GSH}, $OP^{OH\text{-}SLF}$ and $OP^{OH\text{-}DTT}$, which indicates a more pronounced effect of local point sources on these OP endpoints compared to the regional sources. In contrast, $OP^{DTT}v$ showed stronger correlation (r = 0.48 – 0.76, median: 0.62) for most site pairs. Higher correlations for the DTT activity combined with lower CODs suggests that the regional sources such as long-range transport or atmospheric processing could have a larger influence on OP^{DTT} than the local sources.

Methanol-soluble $PM_{2.5}$ OP

In comparison to water-soluble $PM_{2.5}$ OP, CODs for the methanol-soluble OP were generally lower (median: 0.21 – 0.35; Figure 9), indicating higher spatial homogeneity of methanol-soluble PM chemical components that are sensitive to OP. Similar to water-soluble $OP^{DTT}v$, the methanol-soluble $OP^{DTT}v$ showed the lowest COD (0.14 – 0.26, median: 0.21) among five endpoints (Figure 9d), which was consistent with Gao et al. (2017) showing a rather low COD (less than 0.23) for both water-soluble and methanol-soluble OP^{DTT} in Southeast US. Overall, higher correlation coefficients were observed for the methanol-soluble OP (median: 0.41 – 0.67 for different endpoints) than the corresponding water-soluble endpoints (median: 0.13 – 0.62). The correlation coefficients were more elevated for certain endpoints such as $OP^{AA}v$ (r = 0.38 – 0.62, median: 0.46) and $OP^{GSH}v$ (r = 0.23 – 0.65, median: 0.41) than others. It is possible that methanol is able to extract more redox-active PM components coming from ~~common~~ regional emission sources, e.g. biomass burning or secondary organic aerosols, present at these sites. The components originated from these common sources could mask the effect of other components originated from the local sources having a narrower range of solubilities, ~~and~~ thus yielding to an overall lower spatiotemporal variability and better correlation among different sites.

3.~~6~~ 5 Correlations of OP with $PM_{2.5}$ mass concentration

Pearson's r and the slope for simple linear regression of volume-normalized OP activities versus $PM_{2.5}$ mass concentrations were computed for each individual site, and are listed in Table 4. For both water-soluble and methanol-soluble OP, the endpoints of $OP^{AA}v$, $OP^{OH\text{-}SLF}v$ and $OP^{OH\text{-}DTT}v$ were poorly correlated with $PM_{2.5}$ mass ($r < 0.60$ in most cases), while $OP^{GSH}v$ and $OP^{DTT}v$ were moderately-to-strongly correlated with $PM_{2.5}$ mass (r = 0.38 – 0.73 for $OP^{GSH}v$, and 0.54 – 0.82 for $OP^{DTT}v$, except at STL). The lower correlation of OP^{AA} and higher correlation of OP^{DTT} are consistent with multiple previous studies comparing these endpoints (Visentin et al., 2016;Yang et al., 2014;Janssen et al., 2014). Decent correlations for $OP^{GSH}v$ and $OP^{DTT}v$ showed that PM mass concentrations can drive these endpoints to some extent at few locations. However, it is important to note that despite these good correlations, the slope of regression for OP vs. $PM_{2.5}$ mass varied a lot among five sampling sites (range for $OP^{GSH}v$ is 0.003 – 0.016 nmol/min/μg, and 0.005 – 0.028 nmol/min/μg for $OP^{DTT}v$), indicating substantial spatiotemporal heterogeneity in the intrinsic potency of the particles to generate ROS at these sites. This is further corroborated by the spatiotemporal variability of $OP^{GSH}m$ and $OP^{DTT}m$ at different sites as shown in Figure 5 and 6. Thus, $PM_{2.5}$ mass concentrations have only a limited role in determining the oxidative levels of the $PM_{2.5}$ at these sites, and OP seems to be largely driven by the PM chemical composition. Given that the current air quality standards across the world focus only on mass concentration of $PM_{2.5}$, these results indicate towards the inadequacy of this mass-centered approach.

3.~~7~~ 6 Intercorrelation among different OP endpoints

We also calculated the correlation coefficient (Pearson's r) for all pairs of different OPv endpoints at each site, which are listed in Table 5. A high correlation coefficient indicates a common source (or a common pool of chemical components) driving the response of those OP endpoints. For water-soluble OP, the intercorrelations among different endpoints were generally poor at urban sites, i.e. CHI, STL, and IND ($r < 0.60$). Correlations were also poor for nearly all pairs of methanol-soluble OP at STL and IND, but CHI showed significantly elevated r values among different OP

endpoints (r = 0.59 – 0.82). Compared to more urbanized sites, the correlations were generally higher at the local sites, i.e. CMP and BON, with r > 0.60 for many pairs of both water-soluble and methanol-soluble OPv. Since both of these sites are located in smaller cities, the sources of redox-active components probably have lesser complexity compared to the major city sites, which have multiple and more complex emission sources. ~~For example~~As discussed in section 3.2, CMP is ~~adjacent to a major road, and thus~~ largely impacted by the vehicular emissions owing to its location adjacent to a major road. Similarly, BON being a rural site is largely impacted by the agricultural emissions with marginal impact from vehicular emissions and other sources such as long-range transport from surrounding cities (Kim et al., 2005;Buzcu-Guven et al., 2007). Thus, a lack of other major sources contributing to components, which can drive these endpoints in different directions through their interactions (i.e. synergistic or antagonistic), leads to the similarity of their responses and hence a good correlation among them at these two sites. Among all OP endpoints, $OP^{OH\text{-}DTT}v$ showed poorest correlations with other endpoints except $OP^{OH\text{-}SLF}v$, with which it was correlated at most sites (i.e. CHI, IND, CMP and BON) for the methanol-soluble extracts (r = 0.66 – 0.84). Since both of these endpoints measure the rate of generation of ·OH, it probably indicates a synergistic role of metals with organic compounds [e.g. Fe with humic-like substances (HULIS), as shown in many previous studies (Yu et al., 2018;Charrier and Anastasio, 2015;Gonzalez et al., 2017;Wei et al., 2018;Ma et al., 2015)] in partly driving the response of both of these endpoints. Note, $OP^{OH\text{-}DTT}$ is a relatively newly developed assay, and there is hardly any previous literature on its comparison with other OP endpoints.

Overall, a poor-to-moderate and inconstant intercorrelation trend among different endpoints of both water-soluble and methanol-soluble OP at most sites indicates that all these assays could be deficient from being ideal and measuring a single endpoint is not enough to represent the overall OP activity. Although, the OP endpoints used in our study have covered some of the well-known and important pathways of the *in vivo* oxidative stress caused by $PM_{2.5}$, there are other endpoints (e.g. consumption of cysteine, formation of H_2O_2, etc.), and more assays can be developed in the future. We suggest that a collection of diverse range of OP endpoints, measured separately as done in our study could better capture the role of different PM components and their interactions via different pathways for driving the oxidative levels of the PM in a region. However, it should be noted that our study is not designed to assess and rank the biological relevance of these acellular endpoints, which will require an integration of these and possibly other novel assays involving different routes of oxidative stress, in either toxicological or epidemiological studies.~~measuring a single endpoint is not enough to represent the overall OP activity. The diverse range of OP endpoints used in our study could better capture the role of different PM components and their interactions via different pathways for driving the oxidative levels of the PM in a region~~.

4 Conclusion

We analyzed both water-soluble and methanol-soluble OP of ambient $PM_{2.5}$ in the Midwest US using five different acellular endpoints, including OP^{AA}, OP^{GSH}, $OP^{OH\text{-}SLF}$, OP^{DTT} and $OP^{OH\text{-}DTT}$. The spatiotemporal profiles of all OP endpoints and $PM_{2.5}$ mass concentration were investigated for one-year timescale from May 2018 to May 2019 using the Hi-Vol filter samples collected from five Midwest US sites located in urban, rural, and roadside environments.

Compared to homogeneously distributed $PM_{2.5}$ mass, all OP endpoints showed significant spatiotemporal variations among different seasons and sites. Seasonally, most OP endpoints generally peaked in summer for both water-soluble and methanol-soluble OP. Spatially, the roadside site showed the highest OP levels for most OP endpoints in water-soluble extracts, while there were occasional peaks in methanol-soluble extracts at other urban sites. Our results showed very limited differences in the spatiotemporal profiles between OPm and OPv for most endpoints, indicating a marginal role of $PM_{2.5}$ mass in causing the spatiotemporal variability of OP.

Comparing the OP for water- and methanol-soluble extracts, we observed significantly higher OP levels in methanol extracts than the corresponding water-soluble OP activities. This trend was much stronger for ·OH generation endpoints (i.e. $OP^{OH\text{-}SLF}$ and $OP^{OH\text{-}DTT}$), indicating a substantial contribution of Fe and its organic complexes, which could be more efficiently extracted in methanol. In comparison to water-soluble OP, methanol-soluble OP showed lower spatial heterogeneity, and higher intercorrelations among different endpoints, which is probably attributed to a more efficient extraction of water-insoluble redox-active species in methanol originated from various emission sources at different sites.

The correlations of OP with $PM_{2.5}$ mass showed a diverse range, with certain endpoints such as OP^{AA}, $OP^{OH\text{-}SLF}$ and $OP^{OH\text{-}DTT}$ showing a poor correlation, while other endpoints (i.e. OP^{GSH} and OP^{DTT}) showing a moderate-to-strong correlation. Despite these occasional strong correlations, the sensitivity of all OP endpoints towards mass, indicated by the slope of OP vs. $PM_{2.5}$ mass as well as the intrinsic OP (OPm), varied substantially for all OP endpoints across different sites and seasons, showing only a marginal effect of mass concentrations in controlling the oxidative levels of $PM_{2.5}$. Moreover, relatively poor and inconsistent correlations among different OP endpoints reflected different pathways of various ROS-active $PM_{2.5}$ components for exerting oxidative stress. Since our study cannot comment on the biological relevance of these different pathways, we recommend integrating all these and other assays in toxicological or epidemiological studies, to assess their relative utilities.

Collectively, the results obtained through our study provide~~s~~ a strong rationale to recommend that the different endpoints of OP provide useful and additional information than the mass concentrations, which could be relevant to assess the public health impacts associated with ambient $PM_{2.5}$. Our future studies will explore the contribution of different chemical components and their emission sources in determining the oxidative levels of ambient $PM_{2.5}$ in the Midwest US.

Data availability. The data on OP and mass concentration of ambient $PM_{2.5}$ samples collected in the Midwest US are available upon request from the corresponding author.

Author contribution. HY: collection of $PM_{2.5}$ samples, measurement of OP, data analysis, manuscript organization and writing; JVP: collection of $PM_{2.5}$ samples, manuscript editing and revision; YW: collection of $PM_{2.5}$ samples, manuscript editing and revision; VV: conceptualization of study design and methodology, manuscript organization and editing, and overall project supervision.

Competing Interests. The authors declare that they do not have any competing interests.

Acknowledgements. This material is based upon work supported by the National Science Foundation under Grant No. CBET-1847237. We acknowledge the support from Brent Stephens, Yi Wang, and Will Wetherell for providing us the access to the site in Chicago, Indianapolis and St. Louis, respectively.

References

Abbas, I., Verdin, A., Escande, F., Saint-Georges, F., Cazier, F., Mulliez, P., Courcot, D., Shirali, P., Gosset, P., and Garçon, G.: *In vitro* short-term exposure to air pollution $PM_{2.5-0.3}$ induced cell cycle alterations and genetic instability in a human lung cell coculture model, *Environmental Research*, 147, 146-158, 2016.

Abrams, J. Y., Weber, R. J., Klein, M., Samat, S. E., Chang, H. H., Strickland, M. J., Verma, V., Fang, T., Bates, J. T., and Mulholland, J. A.: Associations between ambient fine particulate oxidative potential and cardiorespiratory emergency department visits, *Environmental Health Perspectives*, 125, 107008, 10.1289/ehp1545, 2017.

Allan, K., Kelly, F., and Devereux, G.: Antioxidants and allergic disease: a case of too little or too much?, *Clinical & Experimental Allergy*, 40, 370-380, 2010.

Apeagyei, E., Bank, M. S., and Spengler, J. D.: Distribution of heavy metals in road dust along an urban-rural gradient in Massachusetts, *Atmospheric Environment*, 45, 2310-2323, https://doi.org/10.1016/j.atmosenv.2010.11.015, 2011.

Araujo, J. A., Barajas, B., Kleinman, M., Wang, X., Bennett, B. J., Gong, K. W., Navab, M., Harkema, J., Sioutas, C., and Lusis, A. J.: Ambient particulate pollutants in the ultrafine range promote early atherosclerosis and systemic oxidative stress, *Circulation Research*, 102, 589-596, 2008.

Ayres, J. G., Borm, P., Cassee, F. R., Castranova, V., Donaldson, K., Ghio, A., Harrison, R. M., Hider, R., Kelly, F., and Kooter, I. M.: Evaluating the toxicity of airborne particulate matter and nanoparticles by measuring oxidative stress potential—a workshop report and consensus statement, *Inhalation Toxicology*, 20, 75-99, 10.1080/08958370701665517, 2008.

Bates, J. T., Weber, R. J., Abrams, J., Verma, V., Fang, T., Klein, M., Strickland, M. J., Sarnat, S. E., Chang, H. H., and Mulholland, J. A.: Reactive oxygen species generation linked to sources of atmospheric particulate matter and cardiorespiratory effects, *Environmental Science & Technology*, 49, 13605-13612, 10.1021/acs.est.5b02967, 2015.

Bates, J. T., Fang, T., Verma, V., Zeng, L., Weber, R. J., Tolbert, P. E., Abrams, J. Y., Sarnat, S. E., Klein, M., and Mulholland, J. A.: Review of acellular assays of ambient particulate matter oxidative potential: Methods and relationships with composition, sources, and health effects, *Environmental Science & Technology*, 53, 4003-4019, 2019.

Baumann, K., Jayanty, R., and Flanagan, J. B.: Fine particulate matter source apportionment for the chemical speciation trends network site at Birmingham, Alabama, using positive matrix factorization, *Journal of the Air & Waste Management Association*, 58, 27-44, 2008.

Becker, S., Dailey, L. A., Soukup, J. M., Grambow, S. C., Devlin, R. B., and Huang, Y.-C. T.: Seasonal variations in air pollution particle-induced inflammatory mediator release and oxidative stress, *Environmental Health Perspectives*, 113, 1032-1038, 10.1289/ehp.7996, 2005.

Borlaza, L. J. S., Weber, S., Jaffrezo, J.-L., Houdier, S., Slama, R., Rieux, C., Albinet, A., Micallef, S., Trébluchon, C., and Uzu, G.: Disparities in particulate matter (PM 10) origins and oxidative potential at a city scale (Grenoble, France)–Part 2: Sources of PM 10 oxidative potential using multiple linear regression analysis and the predictive applicability of multilayer perceptron neural network analysis, *Atmospheric Chemistry and Physics*, 21, 9719-9739, 2021.

Buzcu-Guven, B., Brown, S. G., Frankel, A., Hafner, H. R., and Roberts, P. T.: Analysis and apportionment of organic carbon and fine particulate matter sources at multiple sites in the midwestern United States, *Journal of the Air & Waste Management Association*, 57, 606-619, 2007.

Cachon, B. F., Firmin, S., Verdin, A., Ayi-Fanou, L., Billet, S., Cazier, F., Martin, P. J., Aissi, F., Courcot, D., and Sanni, A.: Proinflammatory effects and oxidative stress within human bronchial epithelial cells exposed to atmospheric particulate matter ($PM_{2.5}$ and $PM_{>2.5}$) collected from Cotonou, Benin, *Environmental Pollution*, 185, 340-351, 2014.

Calas, A., Uzu, G., Kelly, F. J., Houdier, S., Martins, J. M., Thomas, F., Molton, F., Charron, A., Dunster, C., and Oliete, A.: Comparison between five acellular oxidative potential measurement assays performed with detailed chemistry on PM 10 samples from the city of Chamonix (France), *Atmospheric Chemistry and Physics*, 18, 7863-7875, 2018.

Calas, A., Uzu, G., Besombes, J.-L., Martins, J. M., Redaelli, M., Weber, S., Charron, A., Albinet, A., Chevrier, F., and Brulfert, G.: Seasonal variations and chemical predictors of oxidative potential (OP) of particulate matter (PM), for seven urban French sites, *Atmosphere*, 10, 698, 2019.

Cesari, D., Merico, E., Grasso, F. M., Decesari, S., Belosi, F., Manarini, F., De Nuntiis, P., Rinaldi, M., Volpi, F., and Gambaro, A.: Source apportionment of PM2. 5 and of its oxidative potential in an industrial suburban site in South Italy, *Atmosphere*, 10, 758, 2019.

Charrier, J., and Anastasio, C.: On dithiothreitol (DTT) as a measure of oxidative potential for ambient particles: evidence for the importance of soluble transition metals, *Atmospheric Chemistry and Physics*, 12, 11317-11350, 10.5194/acp-12-9321-2012, 2012.

Charrier, J. G., McFall, A. S., Richards-Henderson, N. K., and Anastasio, C.: Hydrogen peroxide formation in a surrogate lung fluid by transition metals and quinones present in particulate matter, *Environmental Science & Technology*, 48, 7010-7017, 10.1021/es501011w, 2014.

Charrier, J. G., and Anastasio, C.: Rates of hydroxyl radical production from transition metals and quinones in a surrogate lung fluid, *Environmental Science & Technology*, 49, 9317-9325, 10.1021/acs.est.5b01606, 2015.

Charrier, J. G., McFall, A. S., Vu, K. K., Baroi, J., Olea, C., Hasson, A., and Anastasio, C.: A bias in the "mass-normalized" DTT response–An effect of non-linear concentration-response curves for copper and manganese, *Atmospheric Environment*, 144, 325-334, 10.1016/j.atmosenv.2016.08.071, 2016.

Cho, A. K., Sioutas, C., Miguel, A. H., Kumagai, Y., Schmitz, D. A., Singh, M., Eiguren-Fernandez, A., and Froines, J. R.: Redox activity of airborne particulate matter at different sites in the Los Angeles Basin, *Environmental Research*, 99, 40-47, 10.1016/j.envres.2005.01.003, 2005.

Chung, M. Y., Lazaro, R. A., Lim, D., Jackson, J., Lyon, J., Rendulic, D., and Hasson, A. S.: Aerosol-borne quinones and reactive oxygen species generation by particulate matter extracts, *Environmental Science & Technology*, 40, 4880-4886, 2006.

Councell, T. B., Duckenfield, K. U., Landa, E. R., and Callender, E.: Tire-wear particles as a source of zinc to the environment, *Environmental science & technology*, 38, 4206-4214, 2004.

Daellenbach, K. R., Uzu, G., Jiang, J., Cassagnes, L.-E., Leni, Z., Vlachou, A., Stefenelli, G., Canonaco, F., Weber, S., and Segers, A.: Sources of particulate-matter air pollution and its oxidative potential in Europe, *Nature*, 587, 414-419, 2020.

Deng, X., Zhang, F., Rui, W., Long, F., Wang, L., Feng, Z., Chen, D., and Ding, W.: $PM_{2.5}$-induced oxidative stress triggers autophagy in human lung epithelial A549 cells, *Toxicology in vitro*, 27, 1762-1770, 2013.

Dominici, F., McDermott, A., Zeger, S. L., and Samet, J. M.: Airborne particulate matter and mortality: timescale effects in four US cities, *American Journal of Epidemiology*, 157, 1055-1065, 2003.

Fang, T., Verma, V., Guo, H., King, L. E., Edgerton, E. S., and Weber, R. J.: A semi-automated system for quantifying the oxidative potential of ambient particles in aqueous extracts using the dithiothreitol (DTT) assay: results from the Southeastern Center for Air Pollution and Epidemiology (SCAPE), *Atmospheric Measurement Techniques*, 8, 471-482, 10.5194/amt-8-471-2015, 2015.

Fang, T., Verma, V., Bates, J. T., Abrams, J., Klein, M., Strickland, M. J., Sarnat, S. E., Chang, H. H., Mulholland, J. A., and Tolbert, P. E.: Oxidative potential of ambient water-soluble $PM_{2.5}$ in the southeastern United States: contrasts in sources and health associations between ascorbic acid (AA) and dithiothreitol (DTT) assays, *Atmospheric Chemistry and Physics*, 16, 3865-3879, 10.5194/acp-16-3865-2016, 2016.

Feng, S., Gao, D., Liao, F., Zhou, F., and Wang, X.: The health effects of ambient $PM_{2.5}$ and potential mechanisms, *Ecotoxicology and Environmental Safety*, 128, 67-74, 10.1016/j.ecoenv.2016.01.030, 2016.

Franco, R., Schoneveld, O., Georgakilas, A. G., and Panayiotidis, M. I.: Oxidative stress, DNA methylation and carcinogenesis, *Cancer Letters*, 266, 6-11, https://doi.org/10.1016/j.canlet.2008.02.026, 2008.

Gao, D., Fang, T., Verma, V., Zeng, L., and Weber, R. J.: A method for measuring total aerosol oxidative potential (OP) with the dithiothreitol (DTT) assay and comparisons between an urban and roadside site of water-soluble and total OP, *Atmospheric Measurement Techniques*, 10, 2821, 2017.

Gao, D., Godri Pollitt, K. J., Mulholland, J. A., Russell, A. G., and Weber, R. J.: Characterization and comparison of PM 2.5 oxidative potential assessed by two acellular assays, *Atmospheric Chemistry and Physics*, 20, 5197-5210, 2020a.

Gao, D., Mulholland, J. A., Russell, A. G., and Weber, R. J.: Characterization of water-insoluble oxidative potential of $PM_{2.5}$ using the dithiothreitol assay, *Atmospheric Environment*, 224, 117327, https://doi.org/10.1016/j.atmosenv.2020.117327, 2020b.

Garçon, G., Dagher, Z., Zerimech, F., Ledoux, F., Courcot, D., Aboukais, A., Puskaric, E., and Shirali, P.: Dunkerque City air pollution particulate matter-induced cytotoxicity, oxidative stress and inflammation in human epithelial lung cells (L132) in culture, *Toxicology in vitro*, 20, 519-528, 2006.

Garg, B. D., Cadle, S. H., Mulawa, P. A., Groblicki, P. J., Laroo, C., and Parr, G. A.: Brake Wear Particulate Matter Emissions, *Environmental Science & Technology*, 34, 4463-4469, 10.1021/es001108h, 2000.

Gietl, J. K., Lawrence, R., Thorpe, A. J., and Harrison, R. M.: Identification of brake wear particles and derivation of a quantitative tracer for brake dust at a major road, *Atmospheric Environment*, 44, 141-146, 2010.

Gildemeister, A. E., Hopke, P. K., and Kim, E.: Sources of fine urban particulate matter in Detroit, MI, *Chemosphere*, 69, 1064-1074, https://doi.org/10.1016/j.chemosphere.2007.04.027, 2007.

Godri, K. J., Harrison, R. M., Evans, T., Baker, T., Dunster, C., Mudway, I. S., and Kelly, F. J.: Increased oxidative burden associated with traffic component of ambient particulate matter at roadside and urban background schools sites in London, *PloS One*, 6, e21961, 10.1371/journal.pone.0021961, 2011.

Gonzalez, D. H., Cala, C. K., Peng, Q., and Paulson, S. E.: HULIS enhancement of hydroxyl radical formation from Fe (II): kinetics of fulvic acid-Fe (II) complexes in the presence of lung antioxidants, *Environmental Science & Technology*, 51, 7676-7685, 2017.

Grevendonk, L., Janssen, B. G., Vanpoucke, C., Lefebvre, W., Hoxha, M., Bollati, V., and Nawrot, T. S.: Mitochondrial oxidative DNA damage and exposure to particulate air pollution in mother-newborn pairs, *Environmental Health*, 15, 1-8, 2016.

Gurgueira, S. A., Lawrence, J., Coull, B., Murthy, G. K., and González-Flecha, B.: Rapid increases in the steady-state concentration of reactive oxygen species in the lungs and heart after particulate air pollution inhalation, *Environmental Health Perspectives*, 110, 749-755, 2002.

Haberzettl, P., O'Toole, T. E., Bhatnagar, A., and Conklin, D. J.: Exposure to fine particulate air pollution causes vascular insulin resistance by inducing pulmonary oxidative stress, *Environmental Health Perspectives*, 124, 1830-1839, 2016.

Hammond, D. M., Dvonch, J. T., Keeler, G. J., Parker, E. A., Kamal, A. S., Barres, J. A., Yip, F. Y., and Brakefield-Caldwell, W.: Sources of ambient fine particulate matter at two community sites in Detroit, Michigan, *Atmospheric Environment*, 42, 720-732, 2008.

Held, K. D., Sylvester, F. C., Hopcia, K. L., and Biaglow, J. E.: Role of Fenton chemistry in thiol-induced toxicity and apoptosis, *Radiation Research*, 145, 542-553, 10.2307/3579272, 1996.

Hu, S., Polidori, A., Arhami, M., Shafer, M., Schauer, J., Cho, A., and Sioutas, C.: Redox activity and chemical speciation of size fractioned PM in the communities of the Los Angeles-Long Beach harbor, *Atmospheric Chemistry and Physics*, 8, 6439-6451, 10.5194/acp-8-6439-2008, 2008.

Hulskotte, J., Denier van der Gon, H., Visschedijk, A., and Schaap, M.: Brake wear from vehicles as an important source of diffuse copper pollution, *Water Science & Technology*, 56, 223-231, 10.2166/wst.2007.456, 2007.

Janssen, N. A., Yang, A., Strak, M., Steenhof, M., Hellack, B., Gerlofs-Nijland, M. E., Kuhlbusch, T., Kelly, F., Harrison, R., and Brunekreef, B.: Oxidative potential of particulate matter collected at sites with different source characteristics, *Science of the Total Environment*, 472, 572-581, 10.1016/j.scitotenv.2013.11.099, 2014.

Jeong, C.-H., Traub, A., Huang, A., Hilker, N., Wang, J. M., Herod, D., Dabek-Zlotorzynska, E., Celo, V., and Evans, G. J.: Long-term analysis of $PM_{2.5}$ from 2004 to 2017 in Toronto: Composition, sources, and oxidative potential, *Environmental Pollution*, 263, 114652, 2020.

Künzli, N., Mudway, I. S., Götschi, T., Shi, T., Kelly, F. J., Cook, S., Burney, P., Forsberg, B., Gauderman, J. W., and Hazenkamp, M. E.: Comparison of oxidative properties, light absorbance, and total and elemental mass concentration of ambient $PM_{2.5}$ collected at 20 European sites, *Environmental Health Perspectives*, 114, 684-690, 10.1289/ehp.8584, 2006.

Kampfrath, T., Maiseyeu, A., Ying, Z., Shah, Z., Deiuliis, J. A., Xu, X., Kherada, N., Brook, R. D., Reddy, K. M., and Padture, N. P.: Chronic fine particulate matter exposure induces systemic vascular dysfunction via NADPH oxidase and TLR4 pathways, *Circulation Research*, 108, 716-726, 2011.

Kaufman, J. A., Wright, J. M., Rice, G., Connolly, N., Bowers, K., and Anixt, J.: Ambient ozone and fine particulate matter exposures and autism spectrum disorder in metropolitan Cincinnati, Ohio, *Environmental Research*, 171, 218-227, https://doi.org/10.1016/j.envres.2019.01.013, 2019.

Kelly, F. J.: Oxidative stress: its role in air pollution and adverse health effects, *Occupational and Environmental Medicine*, 60, 612-616, 2003.

Kim, E., Hopke, P. K., Kenski, D. M., and Koerber, M.: Sources of fine particles in a rural midwestern U.S. Area, *Environmental Science & Technology*, 39, 4953-4960, 10.1021/es0490774, 2005.

Kleinman, M. T., Hamade, A., Meacher, D., Oldham, M., Sioutas, C., Chakrabarti, B., Stram, D., Froines, J. R., and Cho, A. K.: Inhalation of concentrated ambient particulate matter near a heavily trafficked road stimulates antigen-induced airway responses in mice, *Journal of the Air & Waste Management Association*, 55, 1277-1288, 2005.

Kodavanti, U. P., Schladweiler, M. C., Ledbetter, A. D., Watkinson, W. P., Campen, M. J., Winsett, D. W., Richards, J. R., Crissman, K. M., Hatch, G. E., and Costa, D. L.: The spontaneously hypertensive rat as a model of human cardiovascular disease: evidence of exacerbated cardiopulmonary injury and oxidative stress from inhaled emission particulate matter, *Toxicology and Applied Pharmacology*, 164, 250-263, 10.1006/taap.2000.8899, 2000.

Kumagai, Y., Koide, S., Taguchi, K., Endo, A., Nakai, Y., Yoshikawa, T., and Shimojo, N.: Oxidation of proximal protein sulfhydryls by phenanthraquinone, a component of diesel exhaust particles, *Chemical Research in Toxicology*, 15, 483-489, 2002.

Kumar, N., Liang, D., Comellas, A., Chu, A. D., and Abrams, T.: Satellite-based PM concentrations and their application to COPD in Cleveland, OH, *Journal of Exposure Science & Environmental Epidemiology*, 23, 637-646, 2013.

Kundu, S., and Stone, E. A.: Composition and sources of fine particulate matter across urban and rural sites in the Midwestern United States, *Environmental Science: Processes & Impacts*, 16, 1360-1370, 2014.

Lee, C.-W., Lin, Z.-C., Hu, S. C.-S., Chiang, Y.-C., Hsu, L.-F., Lin, Y.-C., Lee, I. T., Tsai, M.-H., and Fang, J.-Y.: Urban particulate matter down-regulates filaggrin via COX2 expression/PGE2 production leading to skin barrier dysfunction, *Scientific Reports*, 6, 27995, 10.1038/srep27995, 2016.

Lee, J. H., and Hopke, P. K.: Apportioning sources of $PM_{2.5}$ in St. Louis, MO using speciation trends network data, *Atmospheric Environment*, 40, 360-377, 2006.

Lee, J. H., Hopke, P. K., and Turner, J. R.: Source identification of airborne $PM_{2.5}$ at the St. Louis-Midwest Supersite, *Journal of Geophysical Research: Atmospheres*, 111, 2006.

Li, N., and Nel, A. E.: Role of the Nrf2-mediated signaling pathway as a negative regulator of inflammation: implications for the impact of particulate pollutants on asthma, *Antioxidants & Redox Signaling*, 8, 88-98, 2006.

Li, Y., Fu, S., Li, E., Sun, X., Xu, H., Meng, Y., Wang, X., Chen, Y., Xie, C., and Geng, S.: Modulation of autophagy in the protective effect of resveratrol on $PM_{2.5}$-induced pulmonary oxidative injury in mice, *Phytotherapy Research*, 32, 2480-2486, 2018.

Lin, M., and Yu, J. Z.: Assessment of interactions between transition metals and atmospheric organics: ascorbic acid depletion and hydroxyl radical formation in organic-metal mixtures, *Environmental Science & Technology*, 54, 1431-1442, 10.1021/acs.est.9b07478, 2020.

Liu, Q., Baumgartner, J., Zhang, Y., Liu, Y., Sun, Y., and Zhang, M.: Oxidative potential and inflammatory impacts of source apportioned ambient air pollution in Beijing, *Environmental Science & Technology*, 48, 12920-12929, 2014.

Liu, W., Xu, Y., Liu, W., Liu, Q., Yu, S., Liu, Y., Wang, X., and Tao, S.: Oxidative potential of ambient $PM_{2.5}$ in the coastal cities of the Bohai Sea, northern China: Seasonal variation and source apportionment, *Environmental Pollution*, 236, 514-528, 2018.

Ma, S., Ren, K., Liu, X., Chen, L., Li, M., Li, X., Yang, J., Huang, B., Zheng, M., and Xu, Z.: Production of hydroxyl radicals from Fe-containing fine particles in Guangzhou, China, *Atmospheric Environment*, 123, 72-78, 10.1016/j.atmosenv.2015.10.057, 2015.

Milando, C., Huang, L., and Batterman, S.: Trends in $PM_{2.5}$ emissions, concentrations and apportionments in Detroit and Chicago, *Atmospheric Environment*, 129, 197-209, 2016.

Moreno, T., Kelly, F. J., Dunster, C., Oliete, A., Martins, V., Reche, C., Minguillón, M. C., Amato, F., Capdevila, M., and de Miguel, E.: Oxidative potential of subway PM2. 5, *Atmospheric Environment*, 148, 230-238, 2017.

Mudway, I., Kelly, F., and Holgate, S.: Oxidative stress in air pollution research, *Free Radical Biology & Medicine*, 151, 2-6, 10.1016/j.freeradbiomed.2020.04.031, 2020.

Mudway, I. S., Duggan, S. T., Venkataraman, C., Habib, G., Kelly, F. J., and Grigg, J.: Combustion of dried animal dung as biofuel results in the generation of highly redox active fine particulates, *Particle and Fibre Toxicology*, 2, 6, 10.1186/1743-8977-2-6, 2005.

Oh, S. M., Kim, H. R., Park, Y. J., Lee, S. Y., and Chung, K. H.: Organic extracts of urban air pollution particulate matter ($PM_{2.5}$)-induced genotoxicity and oxidative stress in human lung bronchial epithelial cells (BEAS-2B cells), *Mutation Research/Genetic Toxicology and Environmental Mutagenesis*, 723, 142-151, https://doi.org/10.1016/j.mrgentox.2011.04.003, 2011.

Paraskevopoulou, D., Bougiatioti, A., Stavroulas, I., Fang, T., Lianou, M., Liakakou, E., Gerasopoulos, E., Weber, R., Nenes, A., and Mihalopoulos, N.: Yearlong variability of oxidative potential of particulate matter in an urban Mediterranean environment, *Atmospheric Environment*, 206, 183-196, 2019.

Pei, Y., Jiang, R., Zou, Y., Wang, Y., Zhang, S., Wang, G., Zhao, J., and Song, W.: Effects of Fine Particulate Matter ($PM_{2.5}$) on Systemic Oxidative Stress and Cardiac Function in ApoE−/− Mice, *International Journal of Environmental Research and Public Health*, 13, 484, 2016.

Perrone, M. R., Bertoli, I., Romano, S., Russo, M., Rispoli, G., and Pietrogrande, M. C.: PM2. 5 and PM10 oxidative potential at a Central Mediterranean Site: Contrasts between dithiothreitol-and ascorbic acid-measured values in relation with particle size and chemical composition, *Atmospheric Environment*, 210, 143-155, 2019.

Pietrogrande, M. C., Perrone, M. R., Manarini, F., Romano, S., Udisti, R., and Becagli, S.: PM10 oxidative potential at a Central Mediterranean Site: Association with chemical composition and meteorological parameters, *Atmospheric Environment*, 188, 97-111, 2018.

Pietrogrande, M. C., Bertoli, I., Manarini, F., and Russo, M.: Ascorbate assay as a measure of oxidative potential for ambient particles: Evidence for the importance of cell-free surrogate lung fluid composition, *Atmospheric Environment*, 211, 103-112, 10.1016/j.atmosenv.2019.05.012, 2019.

Poljšak, B., and Fink, R.: The protective role of antioxidants in the defence against ROS/RNS-mediated environmental pollution, *Oxidative Medicine and Cellular Longevity*, 2014, 2014.

Puthussery, J. V., Zhang, C., and Verma, V.: Development and field testing of an online instrument for measuring the real-time oxidative potential of ambient particulate matter based on dithiothreitol assay, *Atmospheric Measurement Techniques*, 11, 5767-5780, 10.5194/amt-11-5767-2018, 2018.

Qin, G., Xia, J., Zhang, Y., Guo, L., Chen, R., and Sang, N.: Ambient fine particulate matter exposure induces reversible cardiac dysfunction and fibrosis in juvenile and older female mice, *Particle and Fibre Toxicology*, 15, 1-14, 2018.

Rao, X., Zhong, J., Brook, R. D., and Rajagopalan, S.: Effect of particulate matter air pollution on cardiovascular oxidative stress pathways, *Antioxidants & Redox Signaling*, 28, 797-818, 2018.

Risom, L., Møller, P., and Loft, S.: Oxidative stress-induced DNA damage by particulate air pollution, *Mutation Research/Fundamental and Molecular Mechanisms of Mutagenesis*, 592, 119-137, 2005.

Riva, D. R., Magalhães, C. B., Lopes, A. A., Lanças, T., Mauad, T., Malm, O., Valença, S. S., Saldiva, P. H., Faffe, D. S., and Zin, W. A.: Low dose of fine particulate matter ($PM_{2.5}$) can induce acute oxidative stress, inflammation and pulmonary impairment in healthy mice, *Inhalation Toxicology*, 23, 257-267, 10.3109/08958378.2011.566290, 2011.

Rosenthal, F. S., Carney, J. P., and Olinger, M. L.: Out-of-hospital cardiac arrest and airborne fine particulate matter: a case–crossover analysis of emergency medical services data in Indianapolis, Indiana, *Environmental Health Perspectives*, 116, 631-636, 2008.

Rossner, P., Svecova, V., Milcova, A., Lnenickova, Z., Solansky, I., and Sram, R. J.: Seasonal variability of oxidative stress markers in city bus drivers: Part II. Oxidative damage to lipids and proteins, *Mutation Research/Fundamental and Molecular Mechanisms of Mutagenesis*, 642, 21-27, https://doi.org/10.1016/j.mrfmmm.2008.03.004, 2008.

Sørensen, M., Daneshvar, B., Hansen, M., Dragsted, L. O., Hertel, O., Knudsen, L., and Loft, S.: Personal $PM_{2.5}$ exposure and markers of oxidative stress in blood, *Environmental Health Perspectives*, 111, 161-166, 2003.

Saffari, A., Daher, N., Shafer, M. M., Schauer, J. J., and Sioutas, C.: Seasonal and spatial variation in reactive oxygen species activity of quasi-ultrafine particles ($PM_{0.25}$) in the Los Angeles metropolitan area and its association with chemical composition, *Atmospheric Environment*, 79, 566-575, 2013.

Saffari, A., Daher, N., Shafer, M. M., Schauer, J. J., and Sioutas, C.: Seasonal and spatial variation in dithiothreitol (DTT) activity of quasi-ultrafine particles in the Los Angeles Basin and its association with chemical species, *Journal of Environmental Science and Health, Part A*, 49, 441-451, 10.1080/10934529.2014.854677, 2014.

Sancini, G., Farina, F., Battaglia, C., Cifola, I., Mangano, E., Mantecca, P., Camatini, M., and Palestini, P.: Health risk assessment for air pollutants: alterations in lung and cardiac gene expression in mice exposed to Milano winter fine particulate matter ($PM_{2.5}$), *PLoS One*, 9, e109685, 10.1371/journal.pone.0109685, 2014.

Sarnat, S. E., Winquist, A., Schauer, J. J., Turner, J. R., and Sarnat, J. A.: Fine particulate matter components and emergency department visits for cardiovascular and respiratory diseases in the St. Louis, Missouri–Illinois, metropolitan area, *Environmental Health Perspectives*, 123, 437-444, 2015.

Shen, H., Barakat, A., and Anastasio, C.: Generation of hydrogen peroxide from San Joaquin Valley particles in a cell-free solution, *Atmospheric Chemistry and Physics*, 11, 753-765, 10.5194/acp-11-753-2011, 2011.

Son, Y., Mishin, V., Welsh, W., Lu, S.-E., Laskin, J. D., Kipen, H., and Meng, Q.: A novel high-throughput approach to measure hydroxyl radicals induced by airborne particulate matter, *International Journal of Environmental Research and Public Health*, 12, 13678-13695, 10.3390/ijerph121113678, 2015.

Sun, B., Shi, Y., Li, Y., Jiang, J., Liang, S., Duan, J., and Sun, Z.: Short-term $PM_{2.5}$ exposure induces sustained pulmonary fibrosis development during post-exposure period in rats, *Journal of Hazardous Materials*, 385, 121566, 2020.

Szigeti, T., Dunster, C., Cattaneo, A., Cavallo, D., Spinazzè, A., Saraga, D. E., Sakellaris, I. A., de Kluizenaar, Y., Cornelissen, E. J., and Hänninen, O.: Oxidative potential and chemical composition of $PM_{2.5}$ in office buildings across Europe–The OFFICAIR study, *Environment International*, 92, 324-333, 10.1016/j.envint.2016.04.015, 2016.

Tuet, W. Y., Fok, S., Verma, V., Rodriguez, M. S. T., Grosberg, A., Champion, J. A., and Ng, N. L.: Dose-dependent intracellular reactive oxygen and nitrogen species (ROS/RNS) production from particulate matter exposure: comparison to oxidative potential and chemical composition, *Atmospheric Environment*, 144, 335-344, 2016.

Verma, V., Rico-Martinez, R., Kotra, N., King, L., Liu, J., Snell, T. W., and Weber, R. J.: Contribution of water-soluble and insoluble components and their hydrophobic/hydrophilic subfractions to the reactive oxygen species-generating potential of fine ambient aerosols, *Environmental Science & Technology*, 46, 11384-11392, 10.1021/es302484r, 2012.

Verma, V., Fang, T., Guo, H., King, L., Bates, J., Peltier, R., Edgerton, E., Russell, A., and Weber, R.: Reactive oxygen species associated with water-soluble $PM_{2.5}$ in the southeastern United States: spatiotemporal trends and source apportionment, *Atmospheric Chemistry and Physics*, 14, 12915-12930, 2014.

Vidrio, E., Phuah, C. H., Dillner, A. M., and Anastasio, C.: Generation of hydroxyl radicals from ambient fine particles in a surrogate lung fluid solution, *Environmental Science & Technology*, 43, 922-927, 10.1021/es801653u, 2009.

909 Visentin, M., Pagnoni, A., Sarti, E., and Pietrogrande, M. C.: Urban $PM_{2.5}$ oxidative potential: Importance of chemical
910 species and comparison of two spectrophotometric cell-free assays, *Environmental Pollution*, 219, 72-79,
911 10.1016/j.envpol.2016.09.047, 2016.

912 Wang, Y., Plewa, M. J., Mukherjee, U. K., and Verma, V.: Assessing the cytotoxicity of ambient particulate matter
913 (PM) using Chinese hamster ovary (CHO) cells and its relationship with the PM chemical composition and oxidative
914 potential, *Atmospheric Environment*, 179, 132-141, 10.1016/j.atmosenv.2018.02.025, 2018.

915 Weber, S., Uzu, G., Calas, A., Chevrier, F., Besombes, J.-L., Charron, A., Salameh, D., Ježek, I., Močnik, G., and
916 Jaffrezo, J.-L.: An apportionment method for the oxidative potential of atmospheric particulate matter sources:
917 application to a one-year study in Chamonix, France, *Atmospheric Chemistry and Physics*, 18, 9617-9629, 2018.

918 Weber, S., Uzu, G., Favez, O., Borlaza, L. J., Calas, A., Salameh, D., Chevrier, F., Allard, J., Besombes, J.-L., and
919 Albinet, A.: Source apportionment of atmospheric PM 10 Oxidative Potential: synthesis of 15 year-round urban
920 datasets in France, *Atmospheric Chemistry and Physics Discussions*, 1-38, 2021.

921 Wei, J., Yu, H., Wang, Y., and Verma, V.: Complexation of iron and copper in ambient particulate matter and its
922 effect on the oxidative potential measured in a surrogate lung fluid, *Environmental Science & Technology*, 53, 1661-
923 1671, 2018.

924 Weichenthal, S., Lavigne, E., Evans, G., Pollitt, K., and Burnett, R. T.: Ambient $PM_{2.5}$ and risk of emergency room
925 visits for myocardial infarction: impact of regional $PM_{2.5}$ oxidative potential: a case-crossover study, *Environmental*
926 *Health*, 15, 46, 10.1186/s12940-016-0129-9, 2016a.

927 Weichenthal, S., Shekarrizfard, M., Traub, A., Kulka, R., Al-Rijleh, K., Anowar, S., Evans, G., and Hatzopoulou, M.:
928 Within-city spatial variations in multiple measures of $PM_{2.5}$ oxidative potential in Toronto, Canada, *Environmental*
929 *Science & Technology*, 53, 2799-2810, 2019.

930 Weichenthal, S. A., Lavigne, E., Evans, G. J., Godri Pollitt, K. J., and Burnett, R. T.: Fine particulate matter and
931 emergency room visits for respiratory illness. Effect modification by oxidative potential, *American Journal of*
932 *Respiratory and Critical Care Medicine*, 194, 577-586, 2016b.

933 Wessels, A., Birmili, W., Albrecht, C., Hellack, B., Jermann, E., Wick, G., Harrison, R. M., and Schins, R. P.: Oxidant
934 generation and toxicity of size-fractionated ambient particles in human lung epithelial cells, *Environmental Science*
935 *& Technology*, 44, 3539-3545, 2010.

936 Xiang, S., Yu, Y. T., Hu, Z., and Noll, K. E.: Characterization of dispersion and ultrafine-particle emission factors
937 based on near-roadway monitoring Part II: Heavy duty vehicles, *Aerosol and Air Quality Research*, 19, 2421-2431,
938 2019.

939 Xing, Y.-F., Xu, Y.-H., Shi, M.-H., and Lian, Y.-X.: The impact of $PM_{2.5}$ on the human respiratory system, *Journal*
940 *of Thoracic Disease*, 8, E69-E74, 2016.

941 Xiong, Q., Yu, H., Wang, R., Wei, J., and Verma, V.: Rethinking the dithiothreitol-based particulate matter oxidative
942 potential: measuring dithiothreitol consumption versus reactive oxygen species generation, *Environmental Science &*
943 *Technology*, 51, 6507-6514, 10.1021/acs.est.7b01272, 2017.

944 Xu, Z., Xu, X., Zhong, M., Hotchkiss, I. P., Lewandowski, R. P., Wagner, J. G., Bramble, L. A., Yang, Y., Wang, A.,
945 and Harkema, J. R.: Ambient particulate air pollution induces oxidative stress and alterations of mitochondria and
946 gene expression in brown and white adipose tissues, *Particle and Fibre Toxicology*, 8, 1-14, 2011.

947 Yan, Z., Wang, J., Li, J., Jiang, N., Zhang, R., Yang, W., Yao, W., and Wu, W.: Oxidative stress and endocytosis are
948 involved in upregulation of interleukin-8 expression in airway cells exposed to $PM_{2.5}$, *Environmental Toxicology*, 31,
949 1869-1878, 10.1002/tox.22188, 2016.

950 Yang, A., Jedynska, A., Hellack, B., Kooter, I., Hoek, G., Brunekreef, B., Kuhlbusch, T. A., Cassee, F. R., and Janssen,
951 N. A.: Measurement of the oxidative potential of $PM_{2.5}$ and its constituents: The effect of extraction solvent and filter
952 type, *Atmospheric Environment*, 83, 35-42, 10.1016/j.atmosenv.2013.10.049, 2014.

953 Yang, A., Hellack, B., Leseman, D., Brunekreef, B., Kuhlbusch, T. A., Cassee, F. R., Hoek, G., and Janssen, N. A.:
954 Temporal and spatial variation of the metal-related oxidative potential of $PM_{2.5}$ and its relation to $PM_{2.5}$ mass and
955 elemental composition, *Atmospheric Environment*, 102, 62-69, 2015a.

956 Yang, A., Wang, M., Eeftens, M., Beelen, R., Dons, E., Leseman, D. L., Brunekreef, B., Cassee, F. R., Janssen, N. A.,
957 and Hoek, G.: Spatial variation and land use regression modeling of the oxidative potential of fine particles,
958 *Environmental Health Perspectives*, 123, 1187-1192, 2015b.

959 Yang, A., Janssen, N. A., Brunekreef, B., Cassee, F. R., Hoek, G., and Gehring, U.: Children's respiratory health and
960 oxidative potential of $PM_{2.5}$: the PIAMA birth cohort study, *Occupational & Environmental Medicine*, 73, 154-160,
961 10.1136/oemed-2015-103175, 2016.

962 Yu, H., Wei, J., Cheng, Y., Subedi, K., and Verma, V.: Synergistic and antagonistic interactions among the particulate
963 matter components in generating reactive oxygen species based on the dithiothreitol assay, *Environmental Science &*
964 *Technology*, 52, 2261-2270, 10.1021/acs.est.7b04261, 2018.

965 Yu, H., Puthussery, J. V., and Verma, V.: A semi-automated multi-endpoint reactive oxygen species activity analyzer
966 (SAMERA) for measuring the oxidative potential of ambient $PM_{2.5}$ aqueous extracts, *Aerosol Science and Technology*,
967 54, 304-320, 2020.

968 Yu, S., Liu, W., Xu, Y., Yi, K., Zhou, M., Tao, S., and Liu, W.: Characteristics and oxidative potential of atmospheric
969 $PM_{2.5}$ in Beijing: Source apportionment and seasonal variation, *Science of the Total Environment*, 650, 277-287, 2019.

970 Zhang, Y., Schauer, J. J., Shafer, M. M., Hannigan, M. P., and Dutton, S. J.: Source apportionment of *in vitro* reactive
971 oxygen species bioassay activity from atmospheric particulate matter, *Environmental Science & Technology*, 42,
972 7502-7509, 10.1021/es800126y, 2008.

973 Zhou, J., Ito, K., Lall, R., Lippmann, M., and Thurston, G.: Time-series analysis of mortality effects of fine particulate
974 matter components in Detroit and Seattle, *Environmental Health Perspectives*, 119, 461-466, 2011.

975 Zuo, L., Otenbaker, N. P., Rose, B. A., and Salisbury, K. S.: Molecular mechanisms of reactive oxygen species-related
976 pulmonary inflammation and asthma, *Molecular Immunology*, 56, 57-63,
977 https://doi.org/10.1016/j.molimm.2013.04.002, 2013.

978

Figures and Tables

Table 1. Averages and (± standard deviation) of OP from various control groups (N = 10) analyzed by SAMERA.

Endpoint	Unit	Negative control Average (± standard deviation)	Chemical used as positive control	Positive control Average (± standard deviation)	Coefficient of variation (CoV, %)
OP^{AA}	μM/min	0.18 ± 0.07	1 μM Cu	0.34 ± 0.04	11.8
OP^{GSH}	μM/min	0.26 ± 0.06	1 μM Cu	0.77 ± 0.02	2.6
$OP^{OH\text{-}SLF}$	nM/min	7.69 ± 1.37	2 μM Fe	13.80 ± 0.70	5.1
OP^{DTT}	μM/min	0.48 ± 0.07	0.2 μM PQ	1.84 ± 0.02	1.1
$OP^{OH\text{-}DTT}$	nM/min	0.55 ± 0.07	0.2 μM 5-H-1,4-NQ	15.45 ± 1.19	7.7

Table 2. Seasonal averages (± standard deviation) of $PM_{2.5}$ mass concentrations (unit: $\mu g/m^3$) at our sampling sites.

	CHI	STL	IND	CMP	BON
Summer 2018	11.2 ± 3.2	14.7 ± 3.4	11.9 ± 3.5	11.4 ± 3.9	10.4 ± 2.0
Fall 2018	10.9 ± 3.4	13.1 ± 3.7	11.5 ± 4.2	7.5 ± 4.3	9.7 ± 3.5
Winter 2018	14.6 ± 3.6	11.8 ± 2.8	11.0 ± 2.7	10.0 ± 3.0	8.6 ± 3.0
Spring 2019	12.6 ± 4.2	13.8 ± 4.0	12.2 ± 2.1	11.6 ± 3.1	9.2 ± 2.3

Table 3. Pearson's correlation coefficient (r) and the associated levels of significance (P) between water-soluble and methanol-soluble OPv for different endpoints at five sampling sites. Correlations with r > 0.60 are shown in **bold**. Asterisks - * and ** indicate significant (P < 0.05) and highly significant (P < 0.01) correlations, respectively.

Site	Pearson's r/significance level (P) for OP endpoints OP^{AA}	OP^{GSH}	$OP^{OH\text{-}SLF}$	OP^{DTT}	$OP^{OH\text{-}DTT}$
CHI	0.09	0.34*	0.53**	0.55**	0.40**
STL	0.24	0.11	0.18	0.28	0.38**
IND	0.24	0.40**	0.33*	0.43**	0.21
CMP	0.42**	**0.63****	0.10	**0.74****	0.58**
BON	0.60**	0.52**	0.41**	**0.68****	0.54**

Table 4. Pearson's r, the associated levels of significance (P) and slope for simple linear regression of water-soluble OPv versus $PM_{2.5}$ mass concentration at five sampling sites. Correlations with r > 0.60 are shown in **bold**. All slope values are in *italic*. Asterisks - * and ** indicate significant (P < 0.05) and highly significant (P < 0.01) correlations, respectively.

(a) Water-soluble OP

		CHI	STL	IND	CMP	BON
OP^{AA}	Pearson's r/P	-0.02	0.33*	0.19	0.54**	0.26
	Slope (*nmol/min/μg*)	*0.000*	*0.005*	*0.004*	*0.031*	*0.007*
OP^{GSH}	Pearson's r/P	0.45**	0.34*	0.45**	**0.72****	0.38*
	Slope (*nmol/min/μg*)	*0.005*	*0.003*	*0.005*	*0.016*	*0.005*
$OP^{OH\text{-}SLF}$	Pearson's r/P	0.09	0.26	0.37**	0.43**	0.24
	Slope (*pmol/min/μg*)	*0.041*	*0.107*	*0.128*	*0.277*	*0.165*
OP^{DTT}	Pearson's r/P	**0.62****	0.27	0.55**	**0.82****	**0.63****
	Slope (*nmol/min/μg*)	*0.013*	*0.005*	*0.013*	*0.020*	*0.015*
$OP^{OH\text{-}DTT}$	Pearson's r/P	0.24	0.60**	0.37**	0.51**	0.45**
	Slope (*pmol/min/μg*)	*0.043*	*0.062*	*0.051*	*0.048*	*0.052*

(b) Methanol-soluble OP

		CHI	STL	IND	CMP	BON
OP^{AA}	Pearson's r~~/P~~	0.55**	0.12	0.52**	**0.64****	**0.61****
	Slope (*nmol/min/µg*)	*0.010*	*0.002*	*0.010*	*0.011*	*0.012*
OP^{GSH}	Pearson's r~~/P~~	0.53**	0.38**	0.51**	**0.73****	**0.63****
	Slope (*nmol/min/µg*)	*0.007*	*0.005*	*0.007*	*0.012*	*0.009*
OP^{OH-SLF}	Pearson's r~~/P~~	0.19	0.34*	0.45**	0.48**	0.52**
	Slope (*pmol/min/µg*)	*0.264*	*0.514*	*0.666*	*0.576*	*0.735*
OP^{DTT}	Pearson's r~~/P~~	0.54**	0.49**	**0.61****	**0.79****	**0.61****
	Slope (*nmol/min/µg*)	*0.017*	*0.016*	*0.019*	*0.028*	*0.022*
OP^{OH-DTT}	Pearson's r~~/P~~	0.25	0.44*	0.51**	0.43**	0.50**
	Slope (*pmol/min/µg*)	*0.072*	*0.079*	*0.143*	*0.075*	*0.165*

Table 5. Pearson's correlation coefficient (r) ~~and the associated level of significance (P)~~ among various endpoints of OPv measured at five sampling sites. The values below the diagonal are for water-soluble OPv, while above are for methanol-soluble OPv. Correlations with r > 0.60 are shown in **bold**. Asterisks - * and ** indicate significant (P < 0.05) and highly significant (P < 0.01) correlations, respectively.

(a) CHI

OP endpoint	Pearson's r~~/significance level (P) for OP endpoints~~				
	OP^{AA}	OP^{GSH}	OP^{OH-SLF}	OP^{DTT}	OP^{OH-DTT}
OP^{AA}		**0.66****	0.60**	**0.69****	0.49**
OP^{GSH}	0.32*		0.30	0.45**	0.17
OP^{OH-SLF}	0.09	0.39**		0.53**	**0.82****
OP^{DTT}	0.05	0.40**	0.40**		**0.64****
OP^{OH-DTT}	0.03	0.30	0.48**	0.18	
	OP^{AA}	OP^{GSH}	OP^{OH-SLF}	OP^{DTT}	OP^{OH-DTT}

(b) STL

OP endpoint	Pearson's r~~/significance level (P) for OP endpoints~~				
	OP^{AA}	OP^{GSH}	OP^{OH-SLF}	OP^{DTT}	OP^{OH-DTT}
OP^{AA}		0.40**	0.19	0.50**	0.33*
OP^{GSH}	0.30		0.13	0.36*	0.23
OP^{OH-SLF}	0.51**	0.17		0.17	0.42**
OP^{DTT}	0.28	0.29	0.22		0.57**
OP^{OH-DTT}	0.40**	0.38**	0.53**	0.34*	
	OP^{AA}	OP^{GSH}	OP^{OH-SLF}	OP^{DTT}	OP^{OH-DTT}

(c) IND

OP endpoint	Pearson's r~~/significance level (P) for OP endpoints~~				
	OP^{AA}	OP^{GSH}	OP^{OH-SLF}	OP^{DTT}	OP^{OH-DTT}
OP^{AA}		0.57**	0.54**	**0.62****	0.57**
OP^{GSH}	0.37**		0.59**	0.52**	0.55**
OP^{OH-SLF}	0.32*	0.23		0.44**	**0.84****
OP^{DTT}	0.17	0.42**	0.44**		0.54**
OP^{OH-DTT}	0.08	0.20	0.29*	0.15	
	OP^{AA}	OP^{GSH}	OP^{OH-SLF}	OP^{DTT}	OP^{OH-DTT}

(d) CMP

OP endpoint	Pearson's r/~~significance level (P) for OP endpoints~~				
	OP^{AA}	OP^{GSH}	$OP^{OH\text{-}SLF}$	OP^{DTT}	$OP^{OH\text{-}DTT}$
OP^{AA}		0.55**	0.46**	**0.70****	0.45**
OP^{GSH}	**0.68****		0.30*	**0.69****	0.15
$OP^{OH\text{-}SLF}$	**0.77****	**0.80****		0.37**	**0.66****
OP^{DTT}	**0.80****	**0.73****	0.58**		0.35*
$OP^{OH\text{-}DTT}$	0.02	0.26	0.15	0.29*	
	OP^{AA}	OP^{GSH}	$OP^{OH\text{-}SLF}$	OP^{DTT}	$OP^{OH\text{-}DTT}$

(e) BON

OP endpoint	Pearson's r/~~significance level (P) for OP endpoints~~				
	OP^{AA}	OP^{GSH}	$OP^{OH\text{-}SLF}$	OP^{DTT}	$OP^{OH\text{-}DTT}$
OP^{AA}		**0.66****	**0.77****	**0.70****	**0.61****
OP^{GSH}	**0.85****		**0.68****	0.60**	0.53**
$OP^{OH\text{-}SLF}$	0.57**	**0.64****		**0.69****	**0.78****
OP^{DTT}	0.51**	0.57**	0.30		**0.68****
$OP^{OH\text{-}DTT}$	0.19	0.31*	0.28	0.32*	
	OP^{AA}	OP^{GSH}	$OP^{OH\text{-}SLF}$	OP^{DTT}	$OP^{OH\text{-}DTT}$

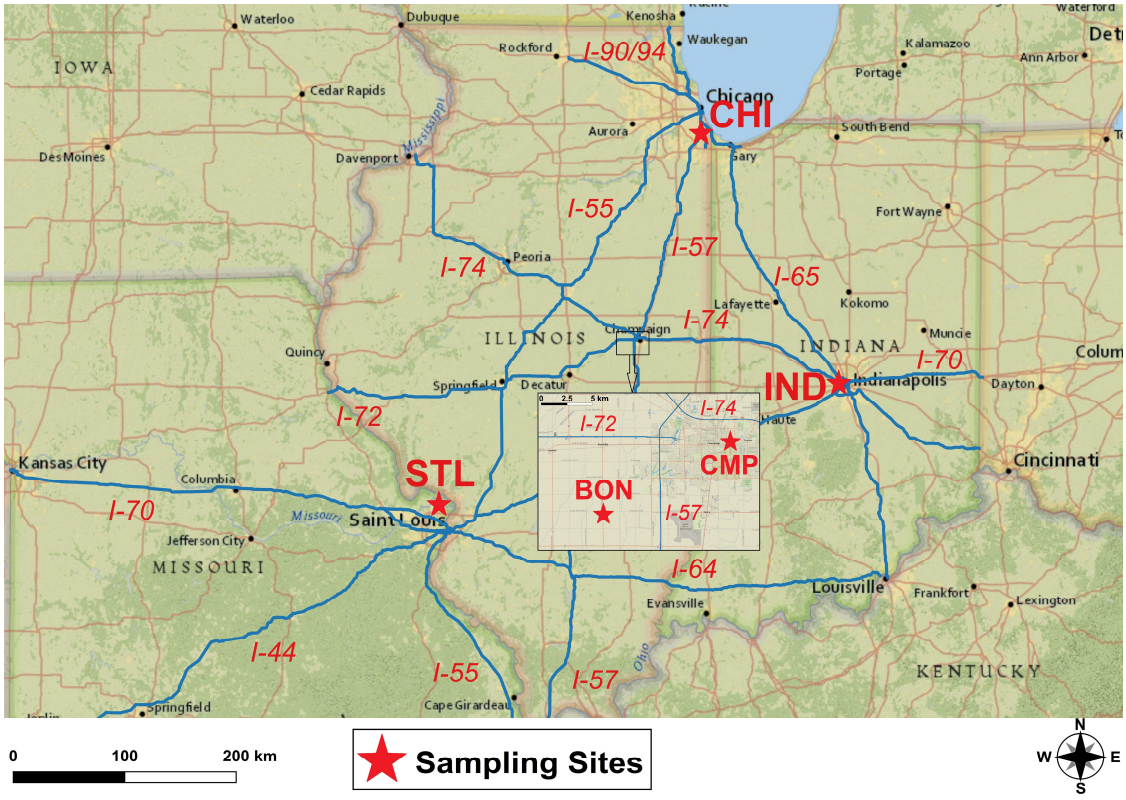

Figure 1. Map for our five sampling sites in the Midwest US.

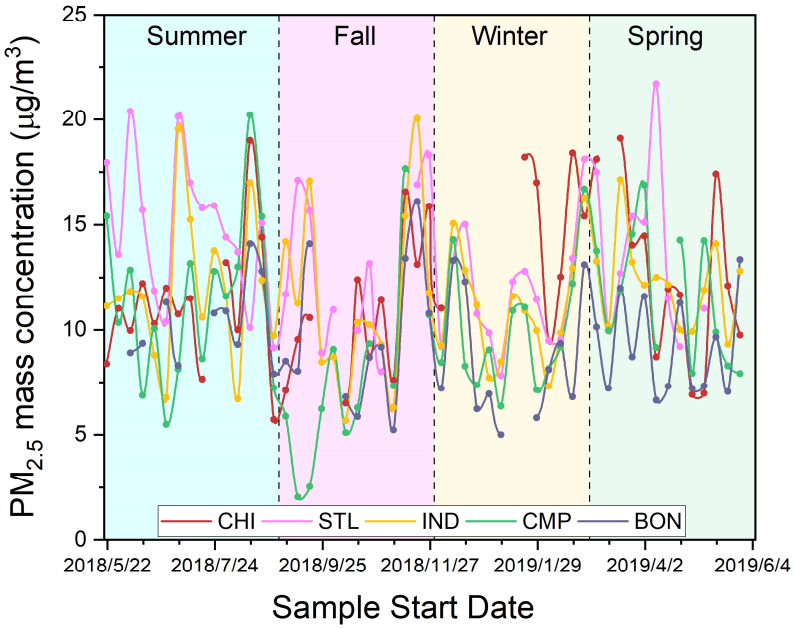

Figure 2. Time series of $PM_{2.5}$ mass concentrations at our sampling sites in the Midwest US.

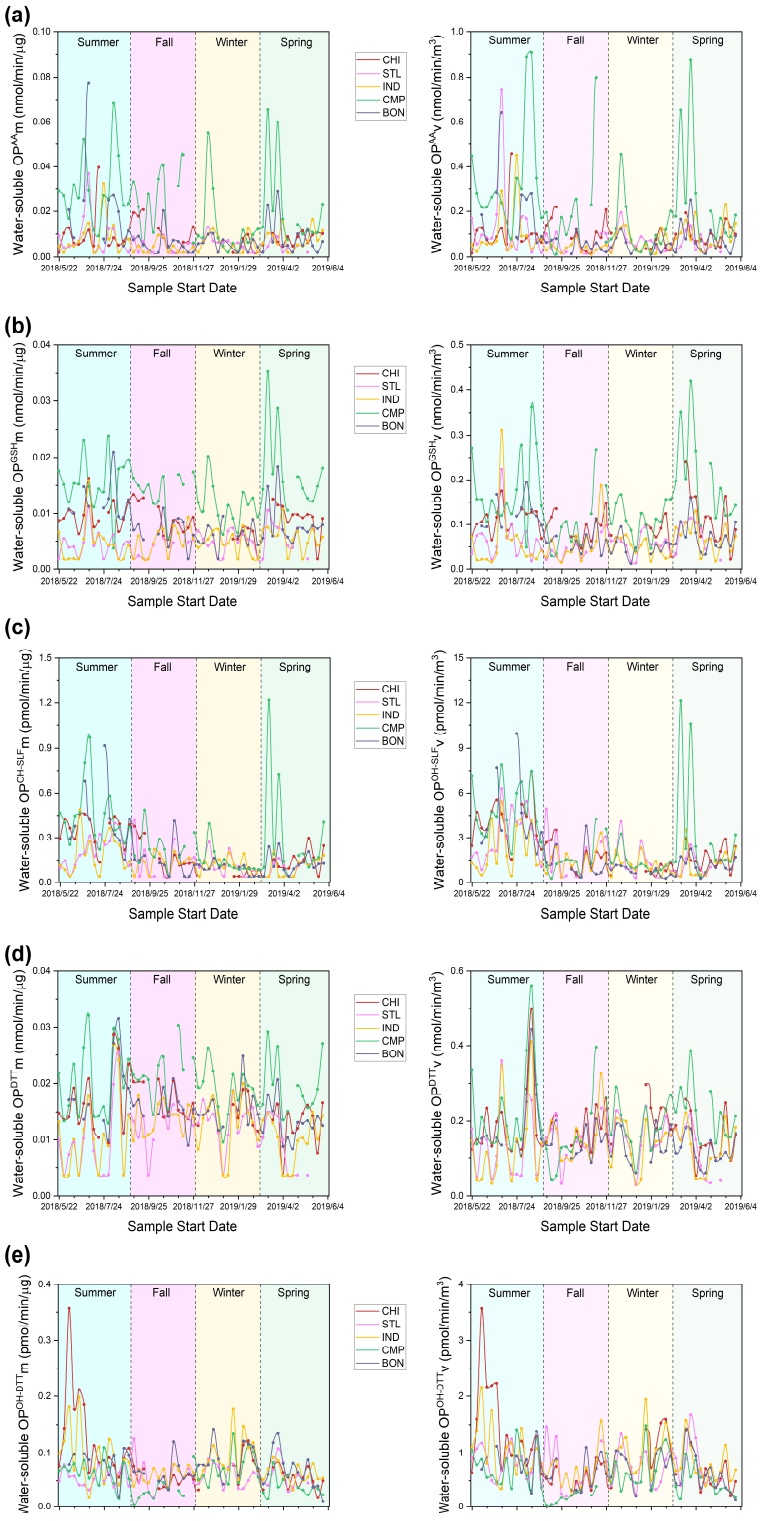

Figure 3. Time series of mass-(left) and volume-(right)normalized water-soluble OP activities for (a) OP^{AA}, (b) OP^{GSH}, (c) $OP^{OH\text{-}SLF}$, (d) OP^{DTT} and (e) $OP^{OH\text{-}DTT}$ at our sampling sites.

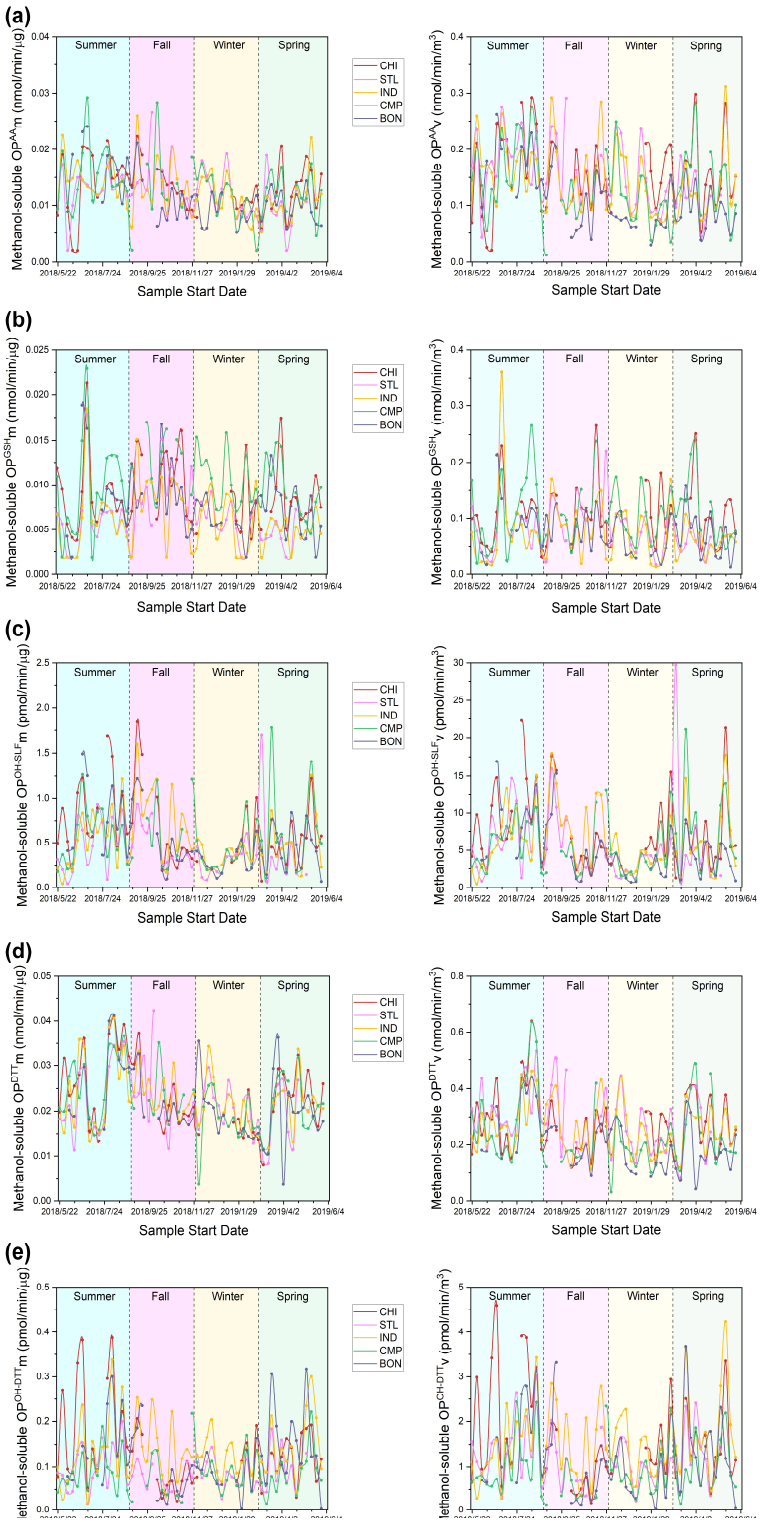

Figure 4. Time series of mass-(left) and volume-(right)normalized methanol-soluble OP activities for (a) OP^{AA}, (b) OP^{GSH}, (c) $OP^{OH\text{-}SLF}$, (d) OP^{DTT} and (e) $OP^{OH\text{-}DTT}$ at our sampling sites.

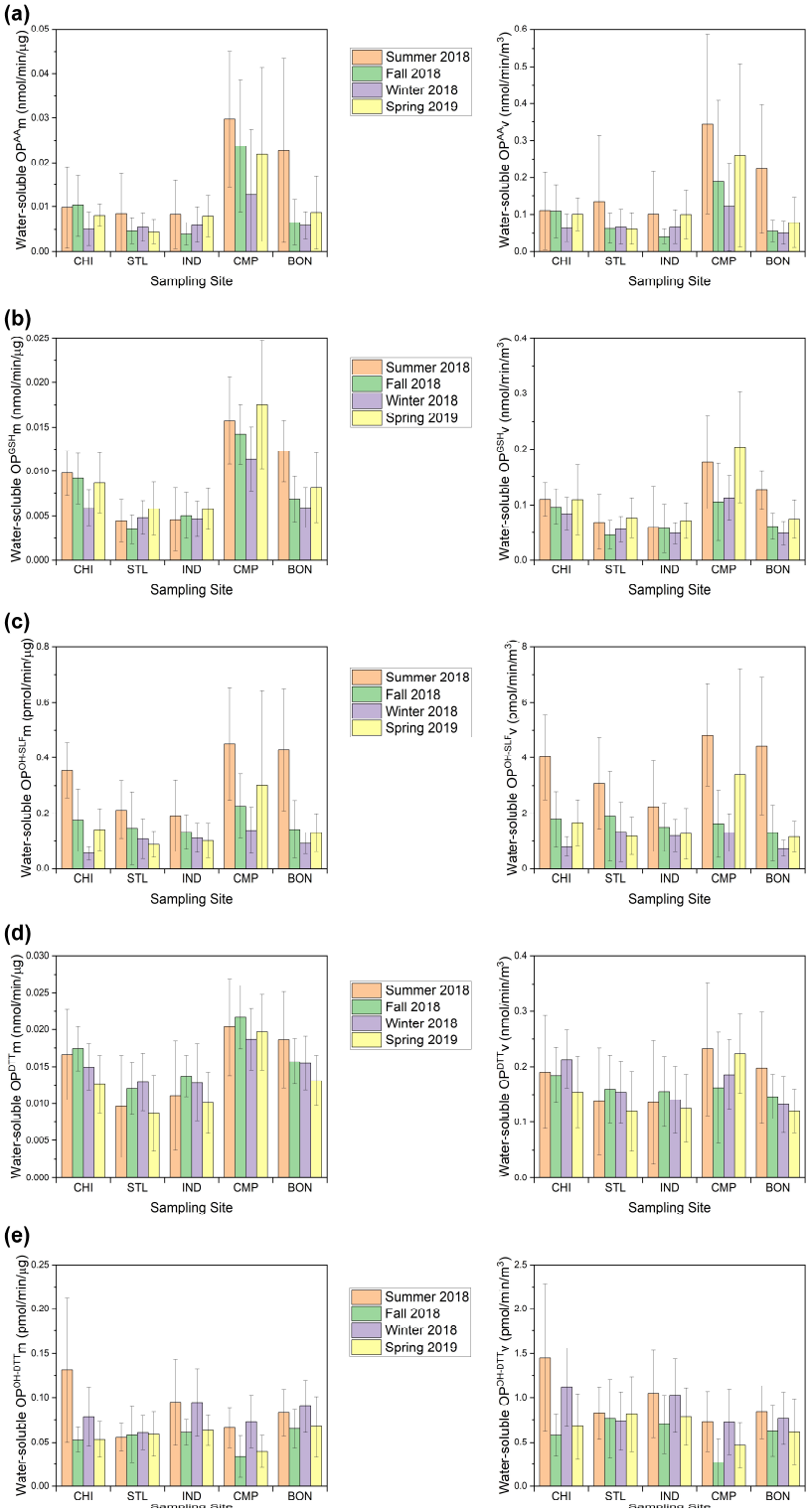

Figure 5. Seasonal averages of mass-(left) and volume-(right) normalized water-soluble OP activities for (a) OP^{AA}, (b) OP^{GSH}, (c) $OP^{OH\text{-}SLF}$, (d) OP^{DTT} and (e) $OP^{OH\text{-}DTT}$ at our sampling sites.

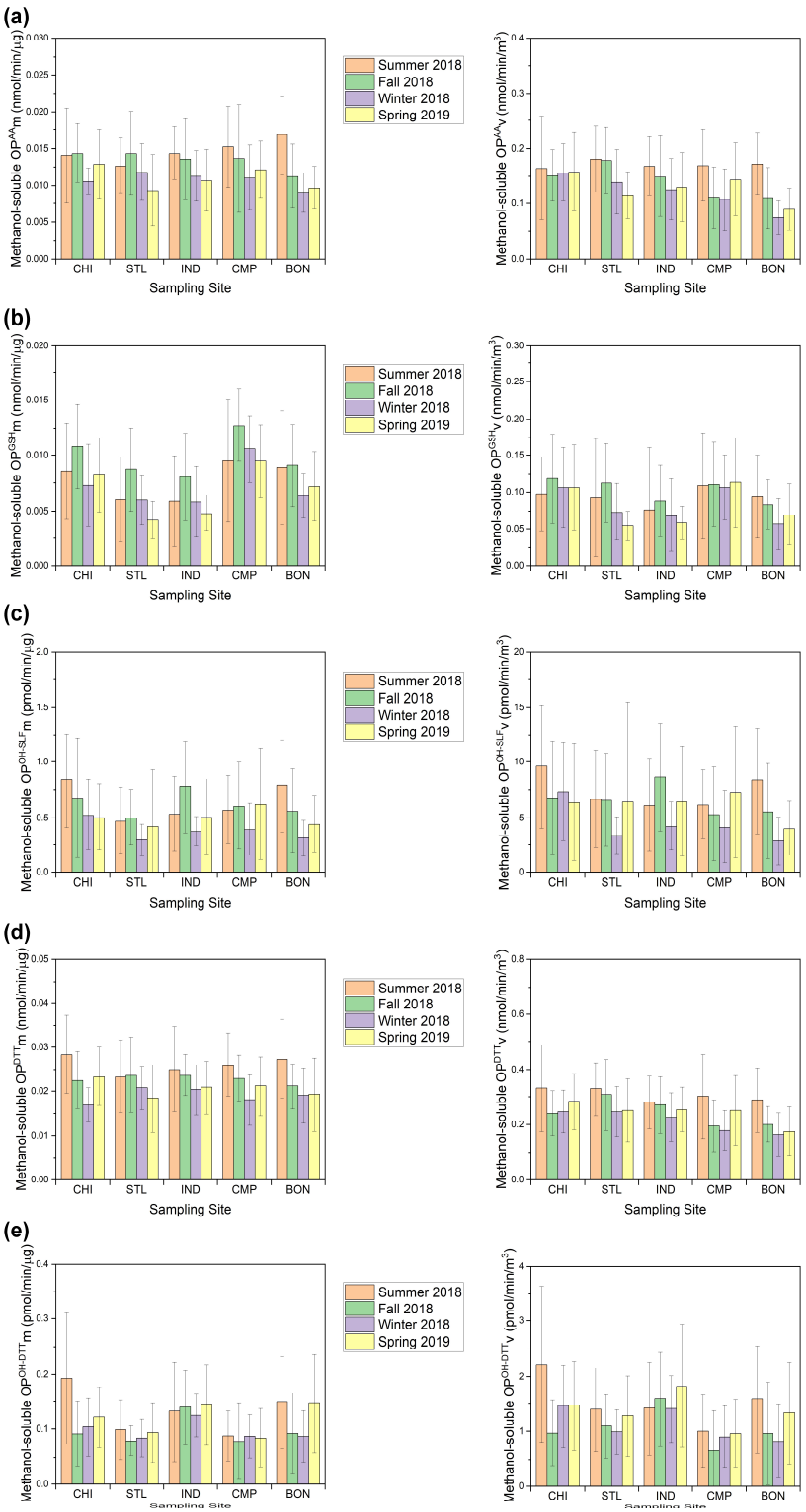

Figure 6. Seasonal averages of mass-(left) and volume-(right) normalized methanol-soluble OP activities for (a) OP^{AA}, (b) OP^{GSH}, (c) $OP^{OH\text{-}SLF}$, (d) OP^{DTT} and (e) $OP^{OH\text{-}DTT}$ at our sampling sites.

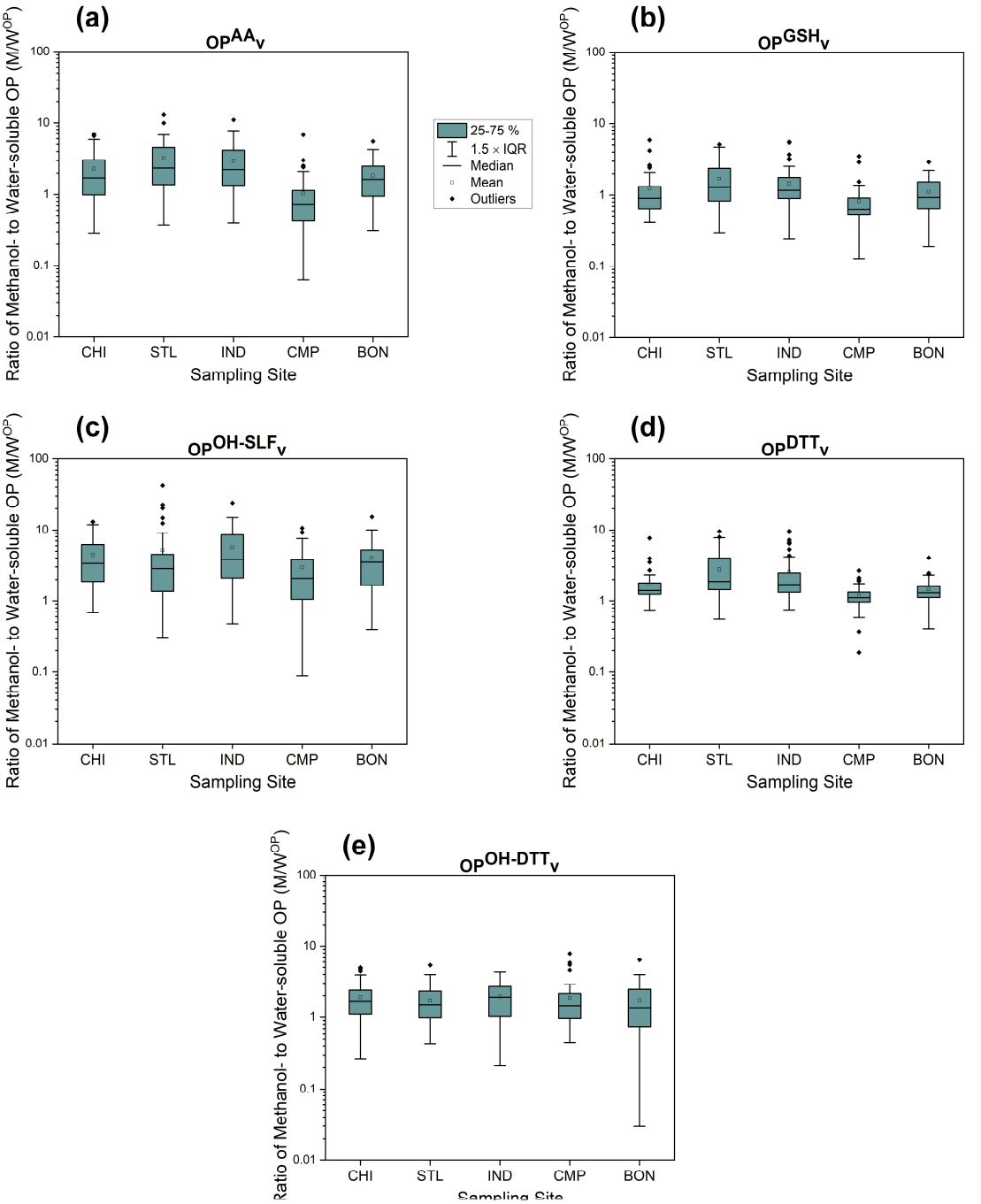

1024

1025 **Figure 7.** Ratio of methanol-soluble OPv to water-soluble OPv (M/W^{OP}) for (a) $OP^{AA}v$, (b) $OP^{GSH}v$, (c)
1026 $OP^{OH\text{-}SLF}v$, (d) $OP^{DTT}v$, and (e) $OP^{OH\text{-}DTT}v$ at five sampling sites.

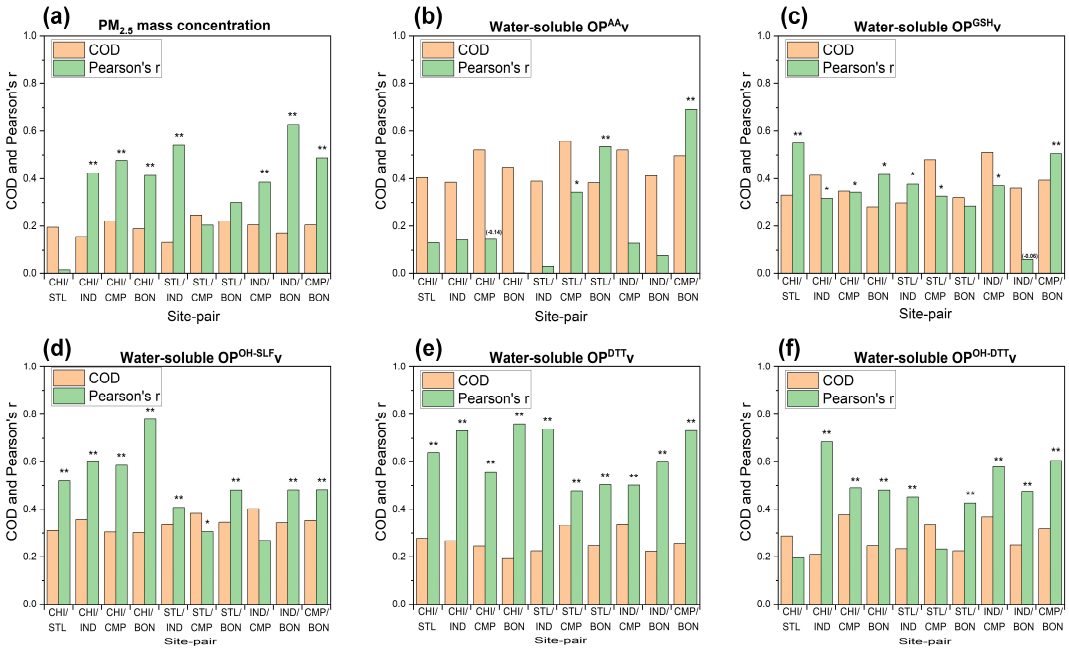

Figure 8. Coefficient of divergence (CoD) and Pearson's r for site-to-site comparison of (a) $PM_{2.5}$ mass and water-soluble OP activities: (b) $OP^{AA}v$, (c) $OP^{GSH}v$, (d) $OP^{OH\text{-}SLF}v$, (e) $OP^{DTT}v$ and (f) $OP^{OH\text{-}DTT}v$. Asterisks - * and ** on the bars of Pearson's r indicate significant ($P < 0.05$) and very significant ($P < 0.01$) correlations, respectively. Note: r for the correlations of $OP^{AA}v$ between CHI and CMP and for the correlations of $OP^{GSH}v$ between IND and BON were negative (-0.14 and -0.06, respectively).

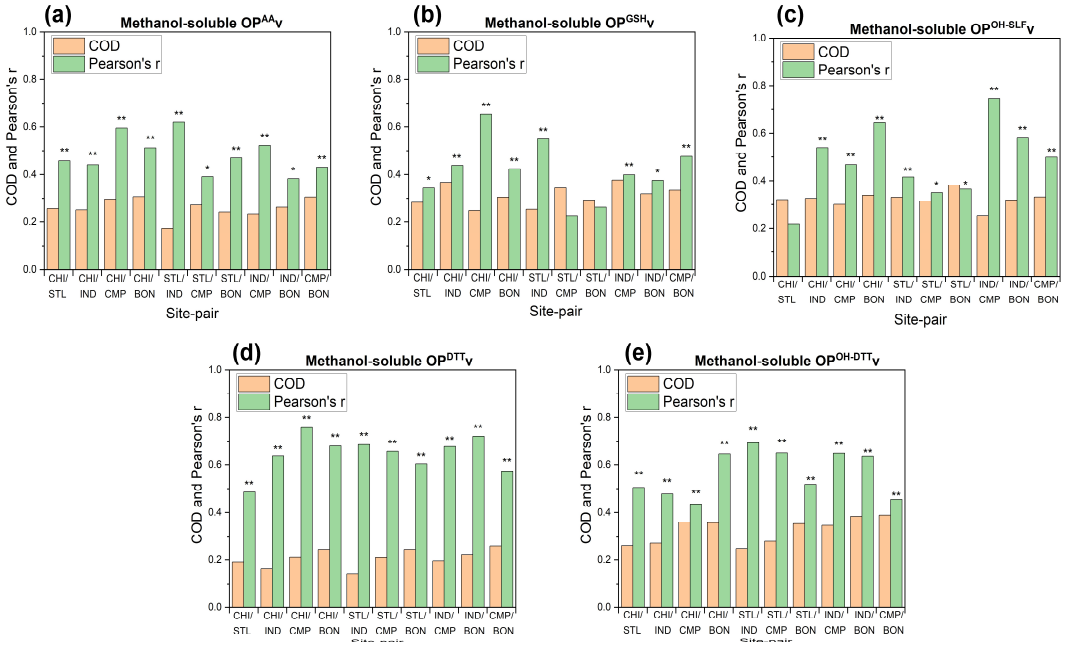

Figure 9. Coefficient of divergence (CoD) and Pearson's r for site-to-site comparison of methanol-soluble OP activities: (a) $OP^{AA}v$, (b) $OP^{GSH}v$, (c) $OP^{OH\text{-}SLF}v$, (d) $OP^{DTT}v$ and (e) $OP^{OH\text{-}DTT}v$. Asterisks - * and ** on the bars of Pearson's r indicate significant ($P < 0.05$) and very significant ($P < 0.01$) correlations, respectively.